Quaternary Science Reviews 141 (2016) 94–111

Contents lists available at ScienceDirect

Quaternary Science Reviews

journal homepage: www.elsevier.com/locate/quascirev

A first chironomid-based summer temperature reconstruction (13–5 ka BP) around 49°N in inland Europe compared with local lake development

Petra Hájková [a, b, *], Petr Pařil [a], Libor Petr [a], Barbora Chattová [a], Tomáš Matys Grygar [c], Oliver Heiri [d]

[a] Department of Botany and Zoology, Faculty of Science, Masaryk University, Kotlářská 2, CZ-61137, Brno, Czech Republic
[b] Department of Vegetation Ecology, Institute of Botany, Academy of Sciences of the Czech Republic, Lidická 25/27, CZ-602 00, Brno, Czech Republic
[c] Institute of Inorganic Chemistry, Academy of Science of the Czech Republic, CZ-25068, Řež, Czech Republic
[d] Institute of Plant Sciences and Oeschger Centre for Climate Change Research, Altenbergrain 21, CH-3013, Bern, Switzerland

ARTICLE INFO

Article history:
Received 27 January 2016
Received in revised form
1 April 2016
Accepted 2 April 2016
Available online 23 April 2016

Keywords:
Carpathians
Climate
Diatoms
Geochemistry
Holocene
Lake-productivity
Late Glacial
Pollen
Transfer functions
Water level changes

ABSTRACT:

Temperature reconstructions for the end of the Pleistocene and the first half of the Holocene based on biotic proxies are rare for inland Europe around 49°N. We analysed a 7 m long sequence of lake deposits in the Vihorlat Mts in eastern Slovakia (820 m a.s.l.). Chironomid head capsules were used to reconstruct mean July temperature (T_{July}), other proxies (diatoms, green algae, pollen, geochemistry) were used to reconstruct local environmental changes that might have affected the climate reconstruction, such as epilimnetic total phosphorus concentrations (TP), lake level changes and development of surrounding vegetation. During the Younger Dryas (YD), temperature fluctuated between 7 and 11 °C, with distinct, decadal to centennial scale variations, that agree with other palaeoclimate records in Europe such as $\delta^{18}O$ content in stalagmites or Greenland ice cores. The results indicate that the site was somewhat colder than expected from the general south-to-north YD temperature gradient within Europe, possibly because of north-facing exposition. The warmer phases of the YD were characterised by low water level or even complete desiccation of the lake (12,200–12,400 cal yr BP). At the Late-Glacial/Holocene transition T_{July} steeply increased from from 11 to 15.5 °C (11,700–11,400 cal yr BP) – the highest T_{July} for entire sequence. This rapid climate change was reflected by all proxies as a compositional change and increasing species diversity. The open woodlands of *Pinus*, *Betula*, *Larix* and *Picea* were replaced by broad-leaved temperate forests dominated by *Betula*, later by *Ulmus* and finally by *Corylus* (ca 9700 cal yr BP). At the same time, input of eroded coarse-grained material into the lake decreased and organic matter (LOI) and biogenic silica increased. The Early-Holocene climate was rather stable till 8700 cal yr BP, with temporary decrease in T_{July} around 11,200 cal yr BP. The lake was productive with a well-developed littoral, as indicated by both diatoms and chironomids. A distinct decline of T_{July} to 10 °C between 8700 and 8000 cal yr BP was associated with decreasing chironomid diversity and increasing climate moistening indicated by pollen. Tychoplanktonic and phosphorus-demanding diatoms increased which might be explained by hydrological and land-cover changes. Later, a gradual warming started after 7000 cal yr BP and representation of macrophytes, periphytic diatoms and littoral chironomids increased. Our results suggest that the Holocene thermal maximum was taking place unusually early in the Holocene at our study site, but its timing might be affected by topography and mesoclimate. We further demonstrated that temperature changes had coincided with variations in local hydrology.

1. Introduction

Recent climate changes have stimulated an intense research on past climatic variations and their impact on both biotic and abiotic ecosystem processes. Quaternary climate changes have been reconstructed using isotope composition in long ice-core or marine

Abbreviations: LOI, loss-on-ignition; LG, Late Glacial; T_{July}, mean July temperature; TP, epilimnetic total phosphorus; YD, Younger Dryas.

* Corresponding author. Department of Botany and Zoology, Faculty of Science, Masaryk University, Kotlářská 2, CZ-61137, Brno, Czech Republic.
E-mail address: buriana@sci.muni.cz (P. Hájková).

http://dx.doi.org/10.1016/j.quascirev.2016.04.001
0277-3791/

sequences (e.g. Blockley et al., 2012; Lowe et al., 2008), or, for Europe, by climate model runs driven by changes in past climate forcing factors such as variations in the North Atlantic thermohaline circulation (e.g. Renssen et al., 2012). Climatic changes, recent or pre-historic, are, however, never uniform across different regions (e.g. Heiri et al., 2014a) and spatial variability in climate dynamics may affect large-scale edaphic processes and species distribution. Regional and local climate can substantially deviate from the global models (Mayewski et al., 2004; Feurdean et al., 2014) because of specific topography and landscape settings. Fossil remains of different organisms like pollen, macrofossils, diatoms or chironomids are often used as climate proxies in local and regional reconstructions (e.g. Davis et al., 2003; Buczkó et al., 2013; Heiri et al., 2014a; Väliranta et al., 2014). Generally, they have shown that the Holocene (since ca 11,650 cal yr BP, Walker et al., 2009) is a warm period with relatively stable climatic conditions compared to Pleistocene. At the end of the Late Glacial (LG), summer temperature in Europe increased, partially as a consequence of orbitally-forced summer insolation, which in the northern Hemisphere was the highest in the Early Holocene (Laskar et al., 2004), partially due to changes in other climate forcing and amplifying factors such as greenhouse gas concentrations, ocean current changes and melting of large continental ice sheets (e.g. Clark et al., 2001; Renssen and Isarin, 2001; Menviel et al., 2011). Nevertheless, in Europe there was some variation in climate during the Holocene, even if with lower amplitude than observed in the late Pleistocene. A review of 50 globally-distributed palaeoclimatical records has shown that Holocene climate variations have been larger and more frequent than is commonly recognized (Mayewski et al., 2004). Several periods of rapid climate change (RCC) were revealed, from which two took place in the Early and Middle Holocene (9000–8000 cal yr BP, 6000–5000 cal yr BP). Most of the climate change events in these globally distributed records were characterised by polar cooling, tropical aridity, and major atmospheric circulation changes. Several abrupt short-term oscillations during the Holocene were also recorded by both, oxygen isotopes in ice-sheet cores (Blockley et al., 2012) and biotic proxies (e.g. Magny et al., 2003; Rosén et al., 2001; Davis et al., 2003; Tóth et al., 2012, 2015). The so called 8.2 ka event was the most pronounced temperature change within the Early and Middle Holocene, which was reflected by a decrease in *Corylus* pollen in the fossil record of North Europe (Seppä et al., 2005; Rasmussen et al., 2008) and less frequently also in Central Europe (Tinner and Lotter, 2001; Dudová et al., 2014). Contrary, chironomid-based reconstructions captured this event rarely (Płóciennik et al., 2011; but see Seppä et al., 2007 and Heiri et al., 2003). It is hence likely that this short-term North Atlantic cooling triggered by Laurentide ice-sheet collapse (Wiersma and Renssen, 2006) influenced regional and local summer temperatures and some types of ecosystems only locally and moreover, it appears that some biotic proxies do not consistently reflect this short-term climate oscillation.

A widely used biotic proxy for temperature reconstruction are fossil chironomids in lake sediment records. Chironomids have a rather short life-cycle and relatively high dissemination ability and therefore show a rapid response to changing environment (Brooks et al., 2007). There are numerous stenotopic species within the chironomids which can provide reliable reconstructions of the past environment. Identification is usually possible at the level of genera or species morphotypes, often with known ecological preferences. In the last 15 years, several calibration data-sets were developed for July air temperature (T_{July}) reconstruction in Eurasia (e.g. Brooks and Birks, 2001; Nazarova et al., 2011; Holmes et al., 2011; Heiri et al., 2011, 2014a). In East-Central Europe, there is a gap in knowledge on chironomid-inferred climate from the LG and Holocene periods. Further, even if chironomids are very good indicators of changes in July temperatures, some autogenic processes not triggered by climate can influence chironomid species turnover and thus distort the climate reconstruction. Typically, there is a general positive correlation between temperature and productivity, but lake productivity can increase independently of temperature because of changing nutrient concentrations and it may be difficult to separate these two influences (Velle et al., 2010). Interpretation of quantitative reconstructions should be therefore done with caution and other biotic or abiotic proxies can help to separate potential independent effects of productivity, oxygen and water level changes from climate influence (e.g. Heiri and Lotter, 2005). Geochemical analyses may serve as a proxy for catchment erosion and diatoms and green algae as reliable proxies of trophic conditions (Battarbee et al., 2001). Regional vegetation composition, reconstructed by means of fossil pollen, can characterise lake catchments in terms of potential intensity of erosion, hydrology or biogeochemistry and in addition may indicate coarse-scale climatic changes as well (Davis et al., 2003; Mauri et al., 2015). In this study we covered all these proxies to provide the first chironomid-based temperature reconstruction for inland Europe around 49°N, covering the end of the Pleistocene and the first half of the Holocene, and to compare it with reconstructed local development of the sedimentary environment.

The study site in the Vihorlat Mts (49°N) is situated between a more southerly located site with a chironomid inferred temperature reconstruction in the Eastern Carpathians (Retezat Mts., 45°N; Tóth et al., 2012, 2015) and a more northerly located site in the Polish lowland (52°N; Płóciennik et al., 2011). According to a review by Heiri et al. (2014a), there is a rather high number of sites where July air temperatures are reconstructed based on chironomids in the Alps, British islands and NW Europe, but data are almost missing for the latitude 47–52°N in East-Central Europe. Tátosová et al. (2006) and Hošek et al. (2014) provided some data on fossil chironomid assemblages, but without quantitative T_{July} reconstruction. Thus, this study fills a gap in our knowledge about past climate in East-Central Europe. Moreover, the position of the study site is transitional between oceanic and continental climate influences and thus shifts in atmospheric circulation and pressure changes, e.g. associated with variations in the predominance of North Atlantic oscillation states, may substantially have influence local climate. Combining different proxies, we aim to separate the influence of past climate changes in the study region from independent local processes like autogenic changes in productivity and lake depth. The main aims of our study were: 1) to reconstruct mean July temperatures (T_{July}) based on chironomid assemblages; 2) to reconstruct local environmental conditions and processes like lake productivity and water level changes using diatoms and green algae to control for undesired local effects in climate reconstruction and 3) to reconstruct changes in the lake surrounding using pollen and geochemical methods to detect influence of changing vegetation cover and extent of erosion.

2. Material and methods

2.1. Study site and sediment sampling

The study site named Hypkaňa is located in the westernmost part of the Eastern Carpathians, in the Vihorlat Mts in eastern Slovakia (East-Central Europe; 820 m a.s.l.; 48°54.787′ N, 22°09.814′ E; see Fig. 1). The geological bedrock is formed by neogenic andezite. The recent climate of the region is characterised by mean annual temperatures of 4–6 °C (mean in January −5–−6 °C, mean in July 14–16 °C) and mean annual precipitation of 1000–1200 mm (http://geo.enviroportal.sk/atlassr). The daily mean temperature (long time series of air temperature, 1961–1990)

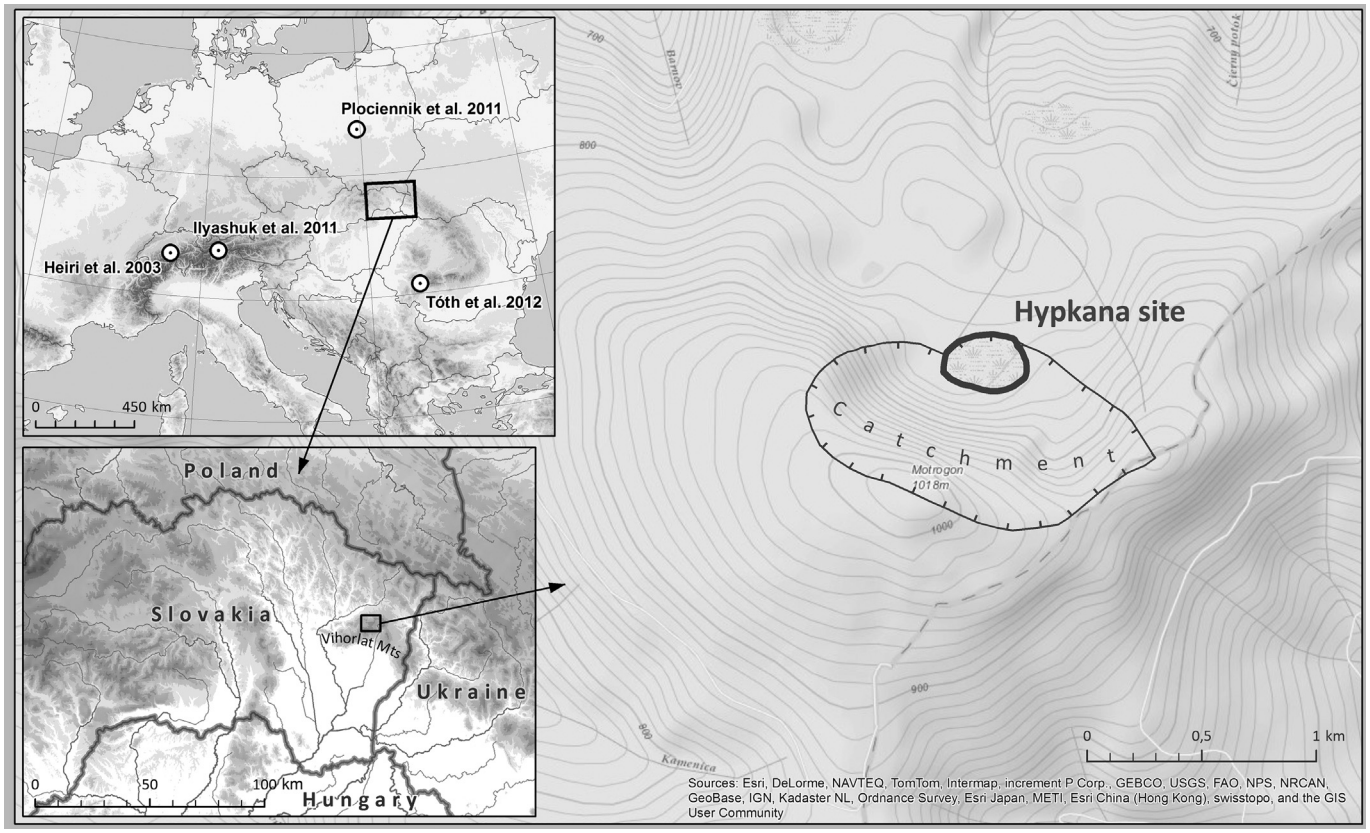

Fig. 1. Position of the study site in Europe and the Carpathian Mts and its geomorphological features and catchment size. The position of some of the sites with T_{July} reconstructions based on chironomids that are discussed in the text are indicated.

in the nearest meteorological station Kamenica nad Cirochou (178 m a.s.l., northern foothills of the Vihorlat Mts) is 18.5 °C, which corrected to 820 m a.s.l. based on a July temperature lapse rate of 0.6 °C/100 m of altitude would be equivalent to 14.7 °C. However, the real temperature of the study site is probably lower because of the northern slope position of the Motrogon Mt (1018 m a. s. l.). The study site has a small catchment area and the present-day mire of ca 2.1 ha has been a Nature Reserve since 1980. The recent vegetation is dominated by *Eriophorum vaginatum, Oxycoccus palustris, Vaccinium myrtillus* and *Molinia caerulea* in the herbaceous layer and *Sphagnum recurvum* agg., *S. magellanicum* and *Polytrichum commune* in the bryophyte layer. The surrounding landscape is overgrown by beech forests and the nearest village Zemplínske Hámre is situated 3.5 km northwards at 400 m a.s.l. The whole profile was 11.1 m deep, of which almost 8 m consisted of lake sediments suitable for chironomid and diatom analyses. The profile was obtained from the central part of the mire in the beginning of May 2012 using combination of a single gouge auger (6 cm diameter, 100 cm length) for the upper slightly decomposed peat sequence and a chamber corer (5 cm diameter, 50 cm length) for limnic sediments analysed in this study. We have sampled two parallel overlapping cores to avoid incomplete recovery.

2.2. Dating and age-depth modelling

Selected macrofossils of terrestrial plants (seeds of taxa specified in Table 1, spindles of *Eriophorum*, bryophytes, *Picea* needles) and ephippia of Cladocera were sent for AMS dating to the Centre for Applied Isotope Studies, University of Georgia, Athens, USA. The IntCal13 calibration curve was used for calibration of ^{14}C dates (Reimer et al., 2013). We obtained altogether 14 radiocarbon dates, from which 11 were used for the depth-age modelling of the entire core including the upper peat layer (see Table 1). Two dates (UG-15694, UG-15690) were excluded because they caused an age reversal and decreased the quality of the model to zero. One date (UG-15689) did not disagree with other ages, but excluding of this date was important for obtaining a reliable Bayesian model with an agreement value at least around 60% (the recommended level). The upper two excluded ^{14}C dates were obtained from macrofossils of mire vegetation (seeds of *Carex rostrata* and *Menyanthes trifoliata*) found in the lake sediment. Likely these macrofossils were transported from the upper layers (by coring or by bioturbation processes) and therefore their ^{14}C date was younger than expected. An age-depth model (Fig. 2) with 1 cm resolution based on a *P_Sequence* function with the k parameter equal to 0.5 cm^{-1} and log10(k/k0) equal to 0.3 was calculated using OxCal 4.2.4. (Bronk Ramsey, 2009). To incorporate potential changes in the sedimentation rate (e.g., contact of different types of deposits), the command *Boundary* was applied. The boundaries were placed at 955 cm (grey gyttja/brown gyttja) and at 323 cm (gyttja/peat). In the text below we use mean values of modelled data in the range of 95.4% and we rounded them to the nearest 50 year step. For the formal subdivision of the Holocene we followed Walker et al. (2012) with the Early-Middle Holocene boundary at 8200 cal yr BP and the Middle-Late Holocene boundary at 4200 cal yr BP.

2.3. Biotic proxies

Samples for pollen analysis (0–800 cm: 1 cm^3, 800–1110 cm: 0.5 cm^3) were treated by acetolysis (Faegri and Iversen, 1989). A minimum of 500 terrestrial pollen grains were counted and determined using pollen keys (Beug, 2004; Reille, 1992). The algae

Table 1
Results of ^{14}C dating (AMS method) from the sediment profile studied. The calibrated ages are median values and intervals of the calibrated 2σ range BP. Dates assigned by asterisk are excluded from the age-depth model.

Samples	Depth (cm)	Dating method	^{14}C age in uncal. BP	Cal yr BP (interval)	Cal yr BP (median)	Material
UG-17161	54–56	AMS	630 ± 25	553–662	597	Bryophytes (*Sphagnum* leaves)
UG-17162	104–106	AMS	2450 ± 25	2361–2701	2526	Spindles (*Eriophorum vaginatum*) + sphagna
UG-17163	174–176	AMS	2770 ± 25	2789–2943	2862	Spindles (*Eriophorum vaginatum*)
UG-19965	214–216	AMS	2870 ± 20	2925–3066	2988	Needles, spindles, bryophytes
UG-15688	265–270	AMS	3380 ± 25	3570–3692	3631	Seeds (*Carex rostrata*)
UG-15689*	320–325	AMS	3510 ± 25	3700–3855	3778	Seeds (*C. rostrata, Menyanthes trifoliata*)
UG-15690*	455–460	AMS	3650 ± 30	3888–4084	3986	Seeds (*Carex rostrata*)
UG-19966	540–545	AMS	6970 ± 50	7689–7930	7802	Ephippia (Cladocera)
UG-15691	700–705	AMS	7930 ± 30	8635–8978	8807	Seed (*Acer* cf. *campestre*)
UG-19968	800–805	AMS	8530 ± 35	9480–9545	9518	Ephippia (Cladocera)
UG-15692	835–840	AMS	8830 ± 30	9709–10,147	9928	Seed (*Picea abies*)
UG-15693	930–935	AMS	9980 ± 45	11,259–11,695	11,477	Ephippia (Cladocera)
UG-15694*	1035–1040	AMS	9780 ± 30	11,181–11,241	11,211	Needles (*Pinus*), seeds (*Betula, Carex* sp.)
UG-15695	1090–1095	AMS	11,020 ± 40	12,749–13,010	12,880	Needles (*Pinus*), ephippia (Cladocera)

of the genus *Pediastrum* and other chlorococcal algae were identified according to Komárek and Jankovská (2001). The nomenclature of all identified pollen types follows Beug (2004). Percentage pollen diagrams were constructed using the total sum (TS) comprising arboreal and non-arboreal pollen. Aquatic and local wetlands plants (including Cyperaceae and *Alnus*), algae and other non-pollen palynomorphs were excluded from the TS. Using *Lycopodium* tablets as a marker we calculated pollen and microcharcoal (fraction 0.01–0.1 mm) concentration and finally pollen and microcharcoal influx.

Sediment samples for chironomid analysis (2–3.5 g of wet weight; 0.8–2.8 g of dry weight) were deflocculated for 20 min in 10% KOH solution (60–75 °C) and then passed through 250 and 100 μm sieves. The chironomid capsules were hand sorted under a stereomicroscope (20–40× magnification) and only specimens consisting of more than half of the mentum were counted. The wet sediments were dried to a constant weight and the number of chironomid remains was calculated to 1 g of dry sediment and identified using Brooks et al. (2007). In all sorted layers (excluding depth 1030–1035 cm) the number of 50 head capsules was reached, which is recommended as a minimum count for the calculation of temperature reconstructions (Heiri and Lotter, 2001). Thus this single layer was excluded from T_{July} reconstruction. Reconstructed T_{July} was re-calculated to T_{July} in 0 m a.s.l. for better comparison with other reconstructions in the literature based on July temperature lapse rates of 0.6 °C/100 m (see e.g. Heiri et al., 2014a). Selected chironomid taxa were classified into ecological categories according to demands on trophic status, bathymetric distribution and preference of macrophytes using relevant literature (Wiederholm, 1983; Brooks et al., 2007; see also Appendix A).

Diatom samples were prepared following the method described in van der Werf (1955). Small quantities of the samples were cleaned by adding 37% H_2O_2 and heating to 80 °C for about 1 h. The reaction was completed by addition of $KMnO_4$. Following digestion and centrifugation, the resulting clean material was diluted with distilled water to avoid excessive concentrations of diatom valves that may hinder reliable observations. Known quantities of *Lycopodium* spores were added to estimate diatom concentrations. Cleaned diatom valves were mounted in Naphrax®, a high-refractive index medium. In each sample, 400 diatom valves were identified and enumerated on random transects at 1,000× magnification using an Olympus B×50 microscope equipped with Differential Interference Contrast (Nomarski) optics. Further, diatoms were classified into five groups according their life form (see also Buczkó et al., 2013 and Appendix B): aerophytic (in subaerial and terrestrial habitats), benthic (at the bottom and shore of the lake), planktonic and tychoplanktonic (in the water column) and periphytic (attached to surfaces).

2.4. Geochemical analyses, LOI, MS

The weight percentage of organic matter was determined by means of loss-on-ignition (LOI) according to Heiri et al. (2001) and Holliday (2004) in each sample. The samples were dried at 105 °C for 24 h, and the combustion at 550 °C took 3 h. Magnetic susceptibility (MS) was determined using a Kappabridge KLY-2 device (Agico, Czech Republic). The results were normalized to get mass-specific magnetic susceptibility in $m^3 \cdot kg^{-1}.10^{-9}$. Magnetic susceptibility provides information about input of eroded clastic sediments (e.g. Shakesby et al., 2007). X-ray fluorescence analysis (EDXRF) of geochemical properties of rocks and soils was carried out using a PANalytical MiniPal4.0 spectrometer with a Peltier-cooled silicon drift energy-dispersive detector. The samples were powdered by agate pestle and mortar and put into measuring cells with a Mylar foil bottom without any further pre-treatment. The analyses were not calibrated and signal counts per second (c.p.s.) of individual elements were evaluated (Grygar et al., 2010). The XRF analytical signal is proportional to element concentrations (Matys Grygar et al., 2014), however, the calibration of this simple XRF setup was not performed: it would depend on matrix effects (element composition, grain size, mean organic matter content), especially in the case of light elements (Al and Si). Matrix effects for such non-destructive XRF analyses are best corrected by using ratios of element signals, such as Zr/Rb or Al/Si.

Because of variable and mostly very high biogenic silica content, the Al/Si ratio, otherwise a versatile proxy of sediment grain size (Grygar et al., 2010; Bouchez et al., 2011) could not be used as it reflects contributions of biogenic silica as well as the grain size trends. The Zr/Rb ratio, another grain size proxy (Jones et al., 2012), can be used to evaluate relative proportions of coarse silt or the finest sand (the typical grain size of zircons, Bouchez et al., 2011) relative to other clastic components, but with negligible influence by autochthonous components. Because in clastic components Zr and Si usually correlate due to their prevalence in coarser size fractions (zircons and quartz), we used Si/Zr as proxy for the relative ratio of biogenic silica to detritic clastics with little lithogenic influence. The Rb/K ratio was used as a proxy for the intensity of chemical weathering, because although both elements are mobilized by chemical weathering, Rb is more strongly retained in clay minerals (illite and smectite) and, hence, in surface sediments it is enriched by chemical weathering (Hu and Gao, 2008).

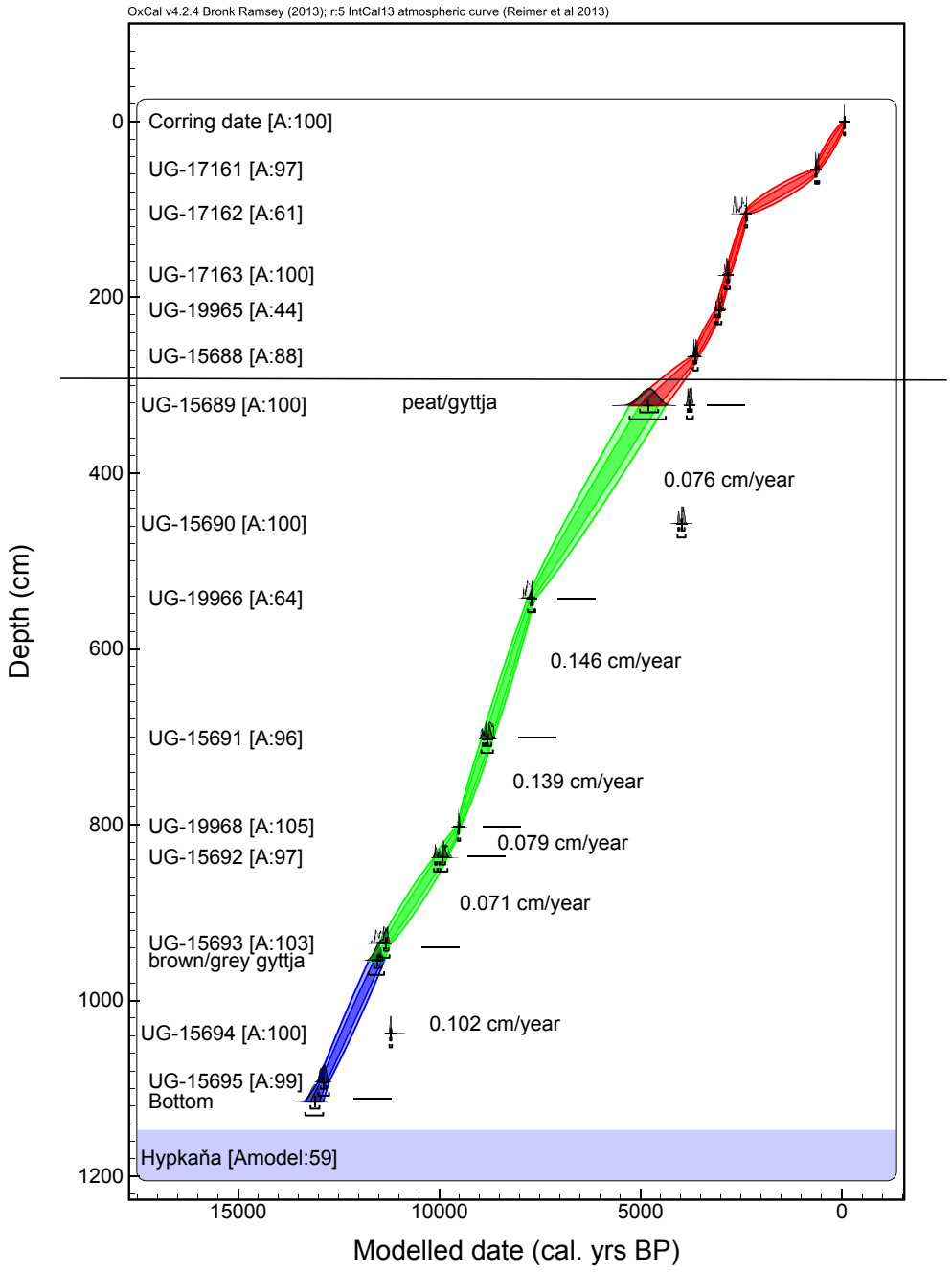

Fig. 2. Age-depth model based on 11 radiocarbon dates. Three dates were excluded from the final model to obtain a reliable Bayesian model with the maximal possible agreement value, which reached 59% between calibrated and modelled dates. The command *Boundary* was used to incorporate sedimentary boundaries, which might change sedimentation rate. Sedimentation rate values are given on the right site of the age-depth curve. The horizontal line indicates the gyttja/peat boundary.

2.5. Data analyses

Species stratigraphic diagrams of chironomids and diatoms as well as a diagram of chemical sediment composition were created using the C2 software (Juggins, 2007). Both, diatom and chironomid counts were converted to percentage data. The pollen percentage diagram was plotted using the Tilia v. 1.7.16 (Grimm, 2011) software. The zonation in pollen, diatom and chironomid diagrams is a result of Coniss cluster analyses with square root transformation of data. To analyse changes in the total species composition of pollen, diatoms and chironomids we used detrended correspondence analyses (DCA) in the Canoco software (ter Braak and Šmilauer, 2002) with down-weighting of rare species, logarithmic transformation of species data and detrending by segments. The length of gradient was 2.14 standard deviation units (SD) for diatoms, 2.08 SD for chironomids and 2.22 by SD for pollen. The variation explained by the first axis was 17.2% for diatoms, 16.1% for chironomids and 28.6% for pollen.

We used an inference model for chironomid-based temperature reconstruction calculated from a Swiss-Norwegian chironomid calibration dataset (Heiri et al., 2011) in order to infer T_{July}. This calibration dataset has been formed by amalgamating two local calibration datasets from Switzerland (Heiri and Lotter, 2010) and Norway (Brooks and Birks, 2001). Altogether, 60 chironomid taxa from the fossil data were used for T_{July} reconstruction. Cold-demanding *Derotanypus* sp. was abundant in some Late-Glacial

layers of the sediment record. In the Swiss calibration dataset head capsules of *Derotanypus* have not been differentiated from other Tanypodinae larvae belonging to *Macropelopia*, *Apsectrotanypus* and *Psectrotanypus*, since all these groups were very rare (max. abundance 2.6%) and often missed glossae, paraglossae and other diagnostic features. Therefore these taxa are also grouped in the Swiss-Norwegian calibration dataset (Heiri et al., 2011). In the absence of other options we assigned *Derotanypus* in the Hypkaňa record to the category *Apsectrotanypus/Derotanypus/Macropelopia/Psectrotanypus* in the calibration data. T_{July} estimates were based on weighted averaging partial least squares (WA-PLS) regression and calibration of square-root- transformed chironomid percentage data. A bootstrapped (cross-validated) root mean squared error of prediction (RMSEP) was 1.4 °C and r^2 0.87 (Heiri et al., 2011).

125 diatom species from the fossil data, which were present also in the calibration datasets, were used to infer epilimnetic total phosphorus (TP) concentrations using diatom-water chemistry transfer functions (Juggins, 2001) based on a combined European diatom data-base (EDDI; http://craticula.ncl.ac.uk/Eddi/jsp). The modern diatom calibration set consists of 477 samples and covers a range of 2–1189 μg TP L^{-1}. The weighted averaging method (WA) and log transformed TP values were used for reconstruction. A jackknifed RMSEP was 0.33 log TP, r^2 0.64, mean bias 0.002 and maximum bias 0.72 log TP. For reconstruction, we used square-root-transformed diatom percentage data.

3. Results and interpretations

3.1. Chronology and sediment description

Using 11 radiocarbon dates we obtained a reliable depth-age model (Fig. 2), which reached the agreement value of 59% between calibrated and modelled values. The sedimentation rate in the lake part of the profile was relatively stable and linear, ranging between 0.07 cm yr^{-1} (in the depth of 935–802 cm and 542–323 cm) and 0.15 cm yr^{-1} (in the depth of 702–542 cm). The error values varied mostly between 50 and 100 years, being only higher (120–220 years) in the depth of 280–500 cm.

The lake sediment (gyttja) accumulated from the LG (ca. 13,000 cal yr BP) up to ca. 4800 cal yr BP. The bottom layer (1115–1037 cm) consisted of light greyish-brown gyttja, the layer 1037–1031 cm of light grey gyttja with admixture of sand, the layer 1031–1002 cm of greyish-brown gyttja with small inorganic admixture with exception of 1025–1022 cm, which was more dark and organic. The layer 1002–955 cm was built up by light greyish-brown gyttja. At 955 cm there was a gradual transition from grey to brown gyttja. The zone 955–920 cm was characterised by alternation of dark and light brown layers. The layer 920–720 cm was built by dark brown gyttja and between 720 and 705 cm there was a gradual transition to brown gyttja (705–531 cm) and light brown gyttja (531–323 cm). For more details see Appendix C.

3.2. Reconstruction of mean July temperature

Pollen analysis confirmed the age depth model for the site and suggested that the record encompassed the entire Younger Dryas (YD) period. The Allerød/YD transition is characterised by a *Betula* pollen decrease, whereas the YD/Early Holocene transition is very clearly distinguished by distinct increase of *Betula* pollen and steep decrease of *Pinus* pollen. Based on the Swiss-Norwegian calibration dataset and inference model for chironomid-based temperature reconstruction, the reconstructed T_{July} oscillated between 7 and 11 °C in the LG (11.8–15.9 °C if corrected to modern sea level; Fig. 3). The lowest T_{July} values were reconstructed at the end of the Allerød period (ca. 13,050–12,950 cal yr BP; 6.9–7.3 °C), at ca. 12,500 cal yr BP (8.5 °C) and at ca. 12,000 cal yr BP (7.6 °C, last cooling). Periods of relatively high temperatures were reconstructed for 12,850–12,600 (9.2–11 °C) and 12,200–12,400 cal yr BP (10.1–10.9 °C). At the end of the YD before the LG/Holocene transition, the first warming up to 10.8 °C was reconstructed (dated to ca. 11,900 cal yr BP in our record). The next warming can be already attributed to the LG/Holocene transition. At 11,600 cal yr BP T_{July} increased to 13.7 °C and at 11,400 cal yr BP to 15.5 °C, which was the highest reconstructed value of T_{July} within the whole Early and Middle Holocene in the study site, although large sections of the interval 11,000–8700 cal yr BP were characterised by very similar temperature values. These temperatures were also higher than recent (1961–1990) mean daily July temperature at the elevation of the study site (14.7 °C). Comparing the course of Holocene temperatures, a distinctly cooler phase was reconstructed between 8700 and 8000 cal yr BP (from 13.9 °C to 10.1–11.1 °C) and at about 7000 cal yr BP (from 12.2 °C to 10.2 °C).

3.3. Lake development in the Late Glacial

Radiocarbon dating suggests that the lake originated at the end of the Allerød interstadial due to landslide activity, which created a dam on the small brook discharging on the hill slopes. Higher abundance of *Betula, Ulmus* and *Quercus* pollen rather confirm this age of origin, however, the rest of pollen spectra do not differ substantially from that typical for YD vegetation. Therefore it may also be possible that the oldest sediment layers originate from the earliest section of the YD interval. The Greenland ice core records indicate that the YD interval started around 12850 cal yr BP which overlaps with our ^{14}C age, but the accuracy of age-depth model in this section is only ca 100 years. In the LG, the lake was a shallow pond as is indicated by chironomids and diatoms (Figs. 4 and 5, zones Hd-1a, 1110–1085 cm, Hch-1a, 1115–1080 cm; 13,100–12,750 cal yr BP). Chironomid assemblages were composed of oligotrophic and cold-demanding taxa such as *Tanytarsus lugens*-type and *Derotanypus* sp., pioneering taxa such as *Corynocera ambigua-type*, semiterrestrial taxa (*Limnophyes* sp.) and chironomids from nearby streams and terrestrial environments (*Georthocladius* sp., *Pseudoorthocladius* sp.). Diatoms were represented by small benthic forms of the genera *Staurosira, Pseudostaurosira and Staurosirella,* which are pioneer species typical for cold oligotrophic lakes with frequent ice cover. Planktonic species (*Asterionella formosa*, *Fragilaria crotonensis*, *Stephanodiscus dubius*) were continually increasing in this developmental zone (Figs. 5 and 6) possibly reflecting increasing water level (cf. also increasing *Tanytarsus lugens*-type, *Chironomus anthracinus*-type). Oligotrophic algae taxa such as *Pediastrum integrum* and *Pediastrum kawraiskyi* were typical for the initial zone (Fig. 6). Around the shallow lake, wetland vegetation dominated by Cyperaceae and *Sphagnum* species developed (Fig. 7, Hp-1). In the next zone (Hd-1b, 1080–1040 cm; Hch-1b; 1075–1040 cm; 12,700–12,400 cal yr BP) evidence suggests that the water depth was continually decreasing and planktonic diatoms were again substituted by small benthic species (*Pseudostaurosira brevistriata*, *Opephora mutabilis*, *Staurosira construens* var. *venter*). At about 1040 cm terrestrial species like *Pinnularia obscura, Pinnularia borealis*, *P. schoenfelderii* and *Microcostatus* cf. *kraskei* indicate dry conditions. Cold-demanding species with high demands for oxygen which can also colonize running waters, occupied (but in low abundances) probably the shallow water of the cold lake or nearby streams (*Heterotrissocladius marcidus-type, Stempellinella* sp.). The next sediment layer (zones Hd-2 + Hch-2, samples in 1030 cm and 1030–1035 cm, respectively, ca 12,300 cal yr BP) suggests total lake desiccation which is indicated by a sole presence of (semi)terrestrial *Limnophyes* sp. with a single head capsule, a species-poor terrestrial

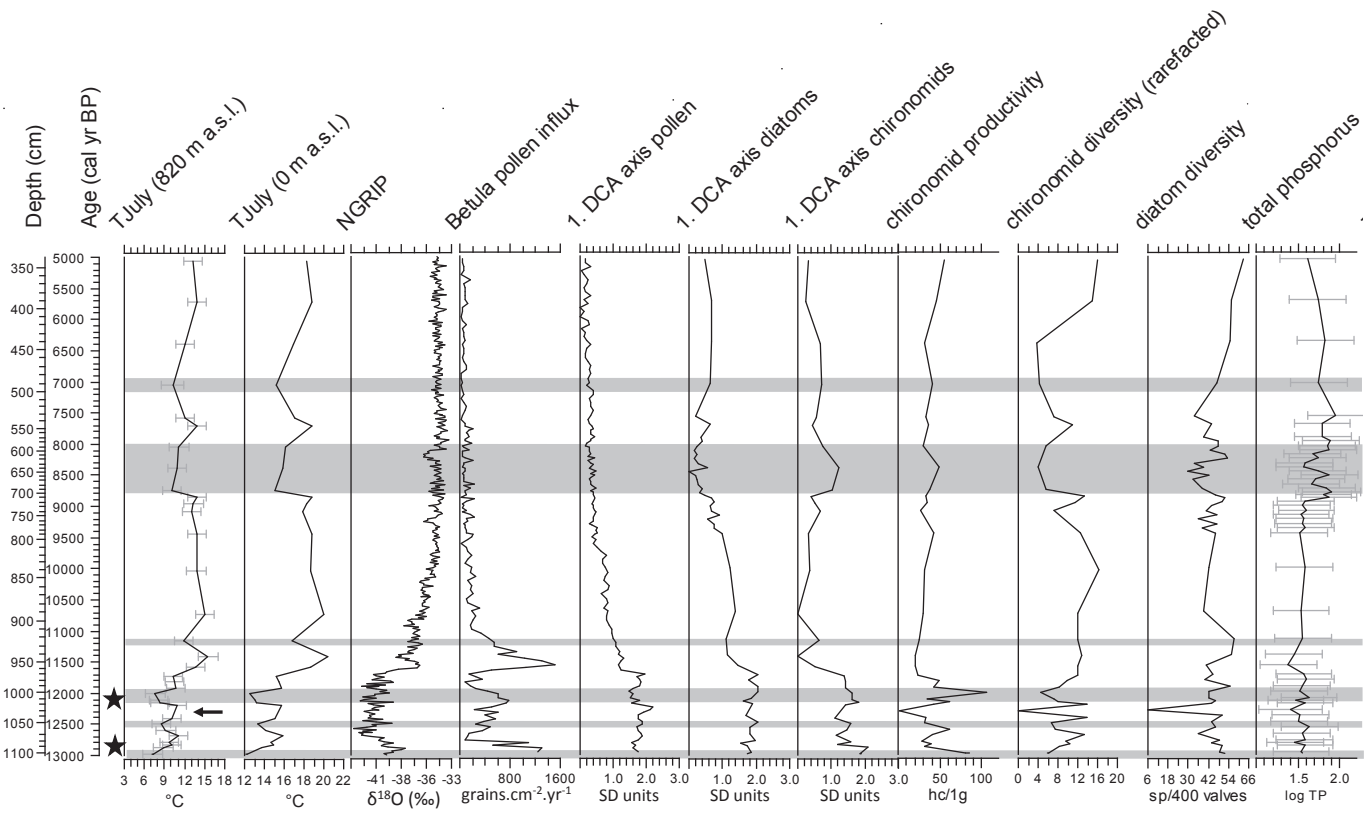

Fig. 3. Results of the chironomid-based T_{July} reconstruction (at 820 m a.s.l. and adjusted to modern sea level using lapse rates of 0.6 °C/100 m), the NGRIP $\delta^{18}O$ record, *Betula* pollen influx, 1st DCA axis of pollen, diatoms and chironomids, chironomid productivity (head capsules per 1 g of dry sediment), chironomid diversity (rarefacted number of taxa), diatom diversity (species per 400 counted valves) and diatom-based epilimnetic total phosphorus. The asterisks indicate layers with *Derotanypus* presence and the arrow indicates the dry layer. The colder periods discussed in the text (low reconstructed T_{July}) are indicated by grey shadings. Data about ^{18}O concentrations from Greenland ice core were obtain from http://www.iceandclimate.nbi.ku.dk/data/ This data file accompanies the following two papers: Seierstad et al. (2014) and Rasmussen et al. (2014).

diatom assemblage (*Hantzschia abundans, H. amphioxys, Pinnularia borealis*) and the almost total absence of green algae (Fig. 6). Hence, the T_{July} reconstruction from this layer was biased and therefore not used. Later (zones Hd-3a + b, Hch-3, 1020–970 cm, 12,200–11,700 cal yr BP), the succession typical for a shallow pond started again with terrestrial chironomid groups (*Smittia* sp.), species typical of cold oligotrophic lakes (*Corynocera ambigua-type*) and taxa tolerating low temperatures (*Derotanypus* sp., *Hydrobaenus* sp., *Stempelinella* sp.). Chironomid assemblages suggest that the water level was gradually increasing, but the lake was probably still shallower than before desiccation. Diatoms indicate gradual restoration of the lake-environment as well as a development of phytoplankton. From ca 1000 cm upwards (12,000 cal yr BP), phytoplankton strongly decreased and it was substituted by small flagilaroid species (*Staurosirella pinnata, Staurosira construents* var. *venter, Opephora mutabilis*). The presence of aerophytic and limnoterrestrial diatoms (*Chamaepinnularia aerophila, Caloneis aerophila*) might indicate either water level decrease, development of a shallow littoral environment or erosion from the surroundings. An increase of macrophytes in the littoral area is also suggested by chironomids (*Cricotopus intersectus*-type, *Tanytarsus pallidicornis*-type).

3.4. Lake development in the Early Holocene

The very beginning of the Holocene (from ca 11,600 cal yr BP onwards) was characterised by the onset or increase of chironomids requiring higher temperatures and higher trophic states (e.g. *Microtendipes pedellus*-type, *Paratanytarsus penicillatus*-type). Groups adapted to cold conditions decreased or even disappeared (*Corynocera ambigua-type*, *Derotanypus* sp., *Zavrelimyia* type A). *Tanytarsus lugens*-type also disappeared for a short time, since the lake had not yet developed an increased water table and deep profundal. Also phytophilic chironomid groups (e.g. *Glyptotendipes pallens*-type, several *Cricotopus* types) occurred in this zone (Hch-4a; 960–890 cm, 11,600–10,700 cal yr BP) and overall chironomid diversity increased steeply (Fig. 3). The green algae assemblage (Fig. 6) is characterised by the disappearance of cold-demanding *Pediastrum kawraiskyi*, decrease of oligotrophic *P. integrum* and steep increase of planktonic *Tetraedron minimum* and *Scenedesmus* sp. Diatom assemblages were characterised by the dominance of planktonic species as well *(Asterionella formosa, Stephanodiscus dubius*). *Stauroneis smithii* was substituted by *S. gracilior.* Local wetland vegetation around the lake consisted of *Alnus* (ca 25% of terrestrial pollen sum) and Cyperaceae, which reached lower abundance than in the previous zone (Fig. 7; Hp-2; 965–925 cm; ca 11,700–11,200 cal yr BP). The presence of macrophytes was indicated by epiphytic diatom taxa (e.g. *Cocconeis pediculus, Cocconeis placentula, Epithemia goeppertiana, E. andata*). Running water taxa, probably coming from a small stream nearby, were present within both, chironomids (*Epoicocladius* sp., *Chaetocladius* sp.) and diatoms (*Planothidium frequentissimum, P. lanceolatum, Reimeria sinnuata*). Even though delimitation of zone 4 is similar for both proxies (960–705 cm for chironomids and 955–720 cm for diatoms; ca 11,600–8950–(8800) cal yr BP), the subzones are positioned differently. Chironomids indicate an earlier change (between 890 and 840 cm), characterised by an increase in abundance of *Cladotanytarsus mancus*-type and *Tanytarsus lugens*-type. The highest

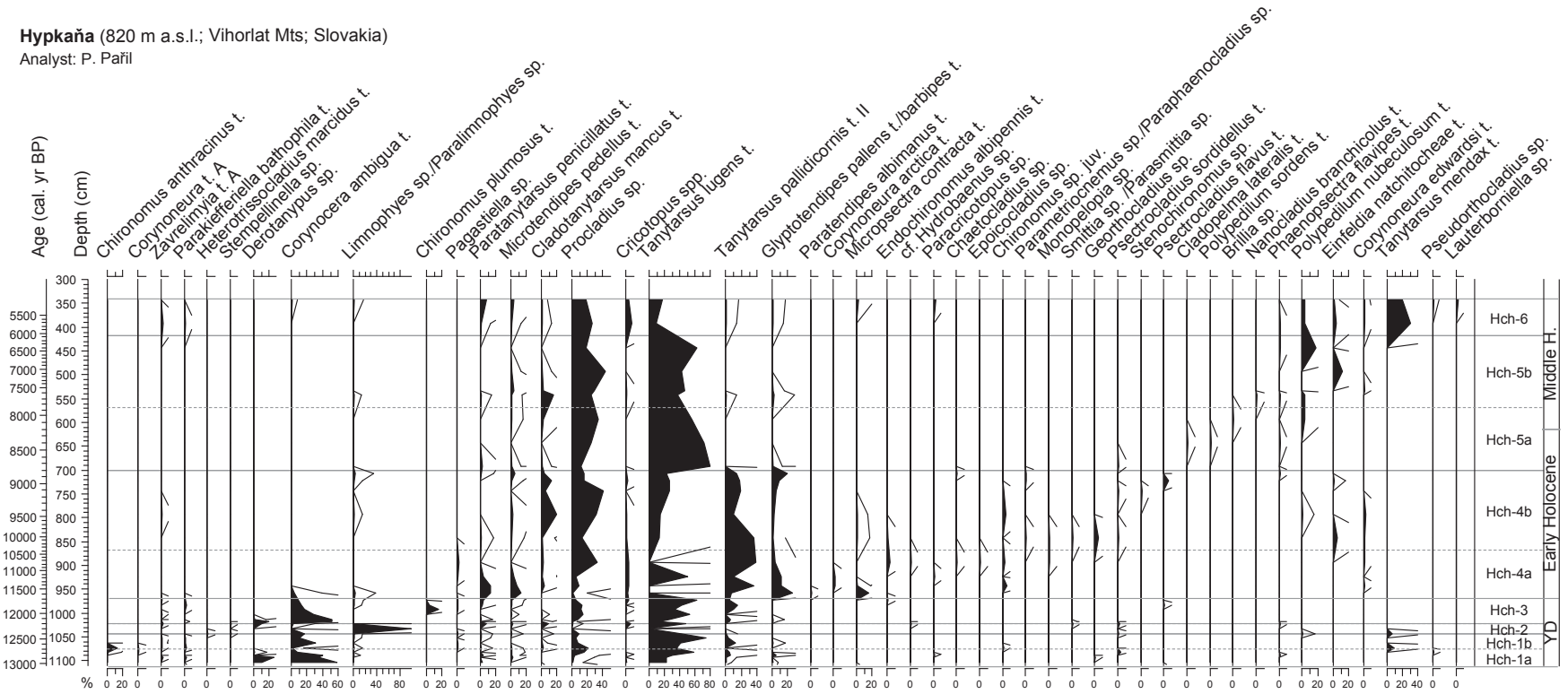

Fig. 4. Stratigraphical diagram of the most important and abundant chironomid morphotypes. The taxa are given in percentages. Rare groups were merged into wider species complexes or to genus level for illustration purposes (but not for quantitative reconstruction). The local chironomid zones are based on results of Coniss cluster analyses with square root transformation of fossil data. Chironomids were identified by P. Pařil (t. = type according Brooks et al., 2007).

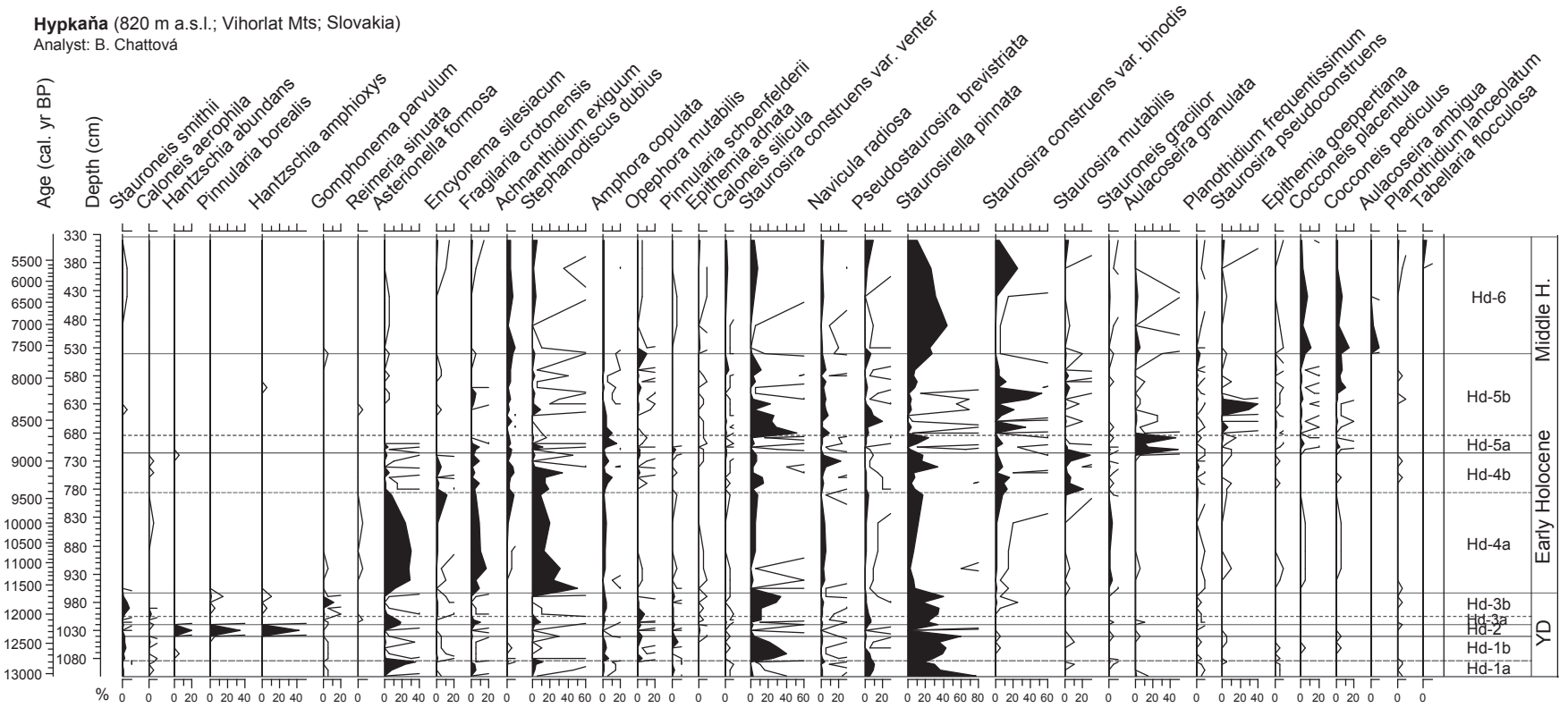

Fig. 5. Stratigraphical diagram of the most important and abundant diatom species. Species are given in percentages. The local diatom zones are based on results of Coniss cluster analyses with square root transformation of fossil data. Diatoms were identified by B. Chattová.

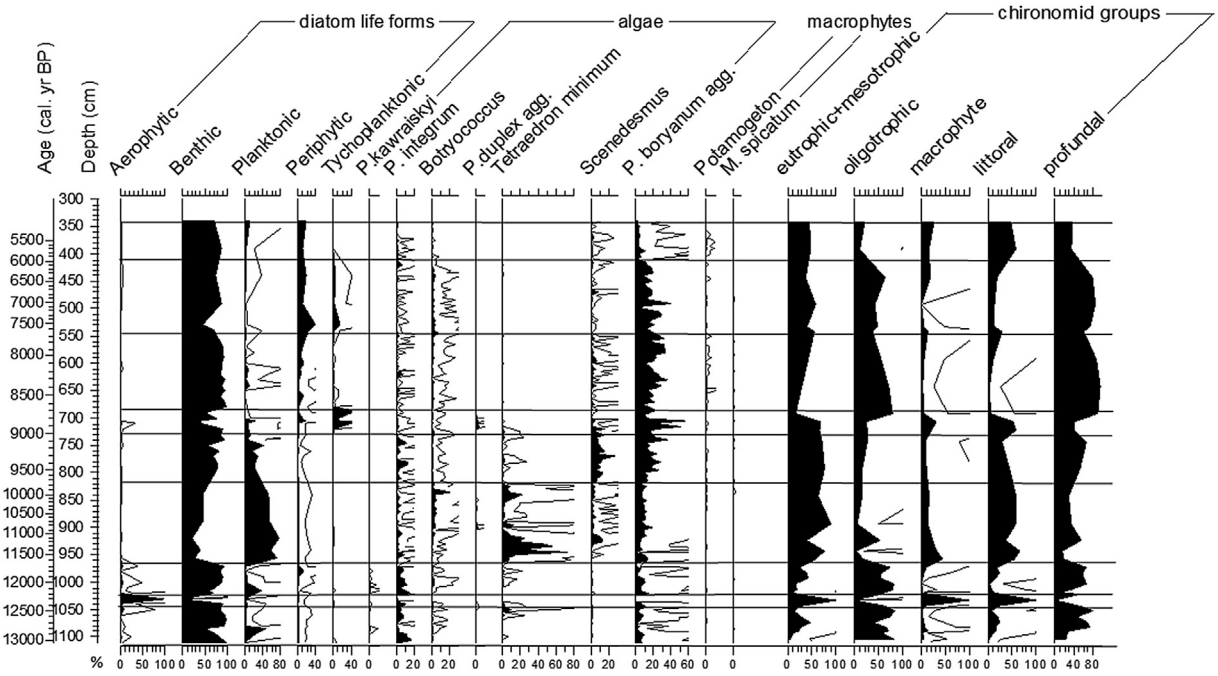

Fig. 6. Summarizing diagram showing representation of different diatom life forms, species of green algae, pollen of macrophytes and chironomid ecological groups. For information about taxa included into particular categories see supplementary material S1 (chironomids) and S2 (diatoms).

diversity of chironomid taxa within the whole profile was recorded at the beginning of the subzone Hch-4b (at about 10,000 cal yr BP). In contrast, a peak in diatom diversity appeared already at the beginning of the subzone Hd-4a (at about 11,500–11,000 cal yr BP), with diversity decreasing thereafter. Diatom species composition indicates distinct change at 790–780 cm (Hd-4a/4b; ca 9400 cal yr BP), where planktonic species (*Asterionella formosa*, *Fragilaria crotonensis*, *Stephanodiscus dubius*) gradually decreased in abundance (Fig. 6) and mesotrophic *Encyonema silesiacum* and *Achnathidium exiiguum* contrarily increased. Simultaneously, the composition of planktonic green algae also changed (at 800 cm; ca 9600 cal yr BP) from an assemblage dominated by *Tetraedron minimum* to dominance of *Scenedesmus.* Abundances of *Pediastrum boryanum* agg. increased. At the end of the subzone Hd-4b, planktonic species almost disappeared and benthic species started to dominate again.

A distinct change in all proxies was apparent at ca 710 cm. In the local terrestrial vegetation, pollen abundance of *Alnus* again increased (Hp-5; 710–430 cm; 8850–6250 cal yr BP). The diatom assemblages of the zone Hd-5a (710–690 cm; 8850–8750 cal yr BP) were characterised by dominance of tychoplanktonic species of the genus *Aulacoseira*, mostly *Aulacoseira granulata.* This species creates hard silicified frustules and therefore it requires an increased degree of turbulence in order to stay in suspension (Saunders et al., 2008). Thus, it indicates turbulent, unstable conditions such as those caused by mixing of water layers by wind (cf. Buczkó et al., 2013). Increased turbulence is almost always associated with increased nutrient flux from the hypolimnion (Stone et al., 2011) which corresponds well with the diatom-inferred TP increase at 710 cm indicating increased trophic state and productivity of autotrophic organisms (diatoms, algae *Pediastrum boryanum* agg., macrophytes). Also chironomids indicate a distinct change in the depth between 710 and 690 cm, even if the reaction to increased phosphorus was apparently not so distinct and the representation of eutrophic (including mesotrophic) and oligotrophic taxa was similar. From the depth of 690 cm onwards, the taxonomic diversity was very low and cold-demanding and profundal-preferring taxa such as *Tanytarsus lugens*-type and *Procladius* sp. started to dominate in the record. Taxa requiring coarse-grained substratum (*Brillia* sp., *Microtendipes pedellus*-type) also occurred (subzone Hch-5a; 695–590 cm; 8750–8050 cal yr BP). Planktonic green algae disappeared (*Tetraedron minimum*) or decreased (*Scenedesmus*; Fig. 6). Also diatom assemblages (subzone Hd-5b; 680–550 cm; 8650–7750 cal yr BP) were characterised by the disappearance of (tycho)-planktonic species and dominance of benthic species (*Amphora copulata, Navicula radiosa*, *Pseudostaurosira brevistriata, Staurosira pseudoconstruens, Staurosira construens* var. *binodis*).

3.5. Lake development in the Middle Holocene

In the chironomid record (subzone Hch-5b; 545–440 cm; 7750–6350 cal yr BP), the more warm-demanding littoral taxa (*Cladotanytarsus mancus*-type) and phytophilic taxa (*Cricotopus* spp., *Glyptotendipes pallens*-type) appeared at the beginning of the Middle Holocene (the beginning of the zone Hch-5b; ca 8000–7600 cal yr BP), but later their abundances again decreased. Towards the end of this zone the abundance of taxa which can colonize sediment or aquatic vegetation (e.g, *Polypedilum nubeculosum*-type) increased, which suggest that the lake may have been shallower and probably over-grown by macrophytes and wetland vegetation (at about 450 cm; 6500 cal yr BP). This is supported also by an increase of *Potamogeton* and Cyperaceae pollen and *Sphagnum* spores (Figs. 6 and 7). In diatom assemblages (lower part of the zone Hd-6; ca 540–430 cm; 7700–6250 cal yr BP), benthic species dominated (e.g. *Staurosirella pinnata*) and were represented at a high diversity. Total diatom species diversity steeply increased (Fig. 3). There was also a higher representation of periphytic (*Cocconeis pediculus*, *Cocconeis placentula*, *Gomphonema* spp.) and tychoplanktonic species (*Aulacoseira ambigua*, *Aulacoseira granulata*) as compared to the previous zone. Finally, the last phase before the complete lake terrestrialization (Hch-6, 395–340 cm, 5750–5050 cal yr BP; Hd-6 – upper part; 390–340 cm; 5700–5050 cal yr BP) was characterised by a decrease in green algae (*Pediastrum boryanum* agg., Fig. 6) and chironomids typical of

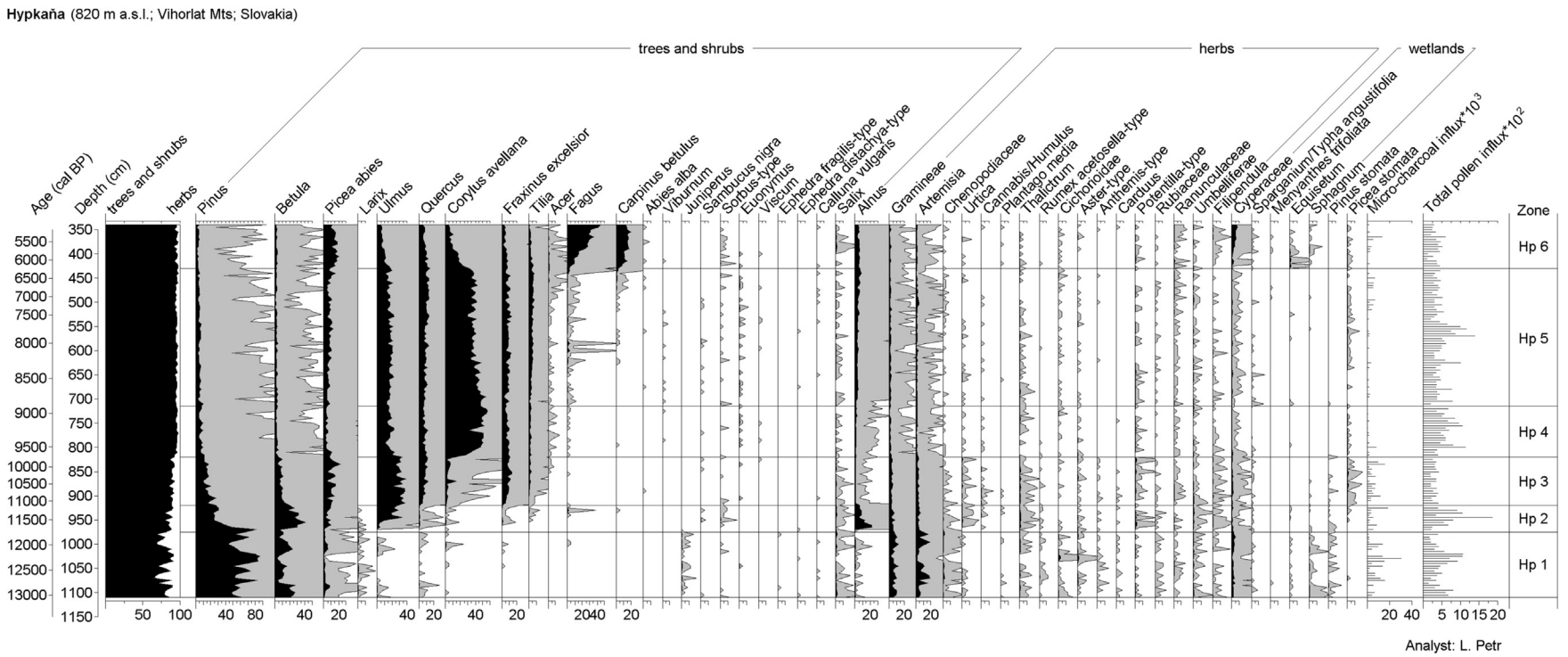

Fig. 7. Pollen percentage diagram with time scale in calibrated years BP (before 1950). At the end of the diagram, microcharcoal particles influx and total pollen influx are given. The local pollen zones are based on results of Coniss cluster analyses with square root transformation of fossil data.

cooler and oligo-to mesotrophic lakes (e.g. *Tanytarsus lugen*-type). Diversity of chironomids and diatoms distinctly increased (Fig. 3). In chironomid assemblages, littoral species (*Polypedilum nubeculosum*-type, *Einfeldia natchitocheae*-type) and groups often associated with vegetation (*Cricotopus* spp.) increased in abundance and ubiquistic groups such as *Tanytarsus mendax*-type started to dominate. In diatom assemblages, species of epibryon (*Tabellaria flocculosa*) and acidophilous species (of the genera *Eunotia, Delicata, Stauroneis, Neidium*) appeared. In the pollen record (Hp-6, 425–345 cm, 6150–5100 cal yr BP), the increase of Cyperaceae pollen and re-appearance of *Sphagnum* spores also indicate spreading of local wetland and mire vegetation.

3.6. Regional vegetation development

The LG forests near the lake were mostly composed of *Pinus* (40–90%) and *Betula* (5–30%) according to fossil pollen spectra and also according to needles and seeds used for AMS dating (Fig. 7; Hp-1; 1110–975 cm; ca 13,050–11,750 cal yr BP). Pollen of other trees and shrubs including the temperate ones (*Picea, Larix, Ulmus* and *Quercus*) were present in lower or very low abundances (*Fagus, Fraxinus* and *Corylus*) and came probably from the lower altitude. *Juniperus*, and *Salix* pollen suggested that in the shrub layer these taxa may have occurred. *Artemisia* and Gramineae were dominant pollen taxa suggesting open steppe or tundra vegetation in the vicinity of the lake, less common were Chenopodiaceae, *Thalictrum*, *Filipendula, Urtica, Rumex acetosella* t. (=type) and steppe species *Ephedra fragilis* t. and *E. distachya* t. The AP/NAP ratio fluctuated between 65 and 90%. Microcharcoal was relatively frequent. After the warming, at the transition between the LG and Early Holocene (Hp-2; 970–920 cm; ca 11,700–11,150 cal yr BP), the pollen percentages of *Pinus* strongly decreased (to 30%), whereas *Betula* (up to 30–40%) and *Alnus* (10–20%) increased. At the end of the zone *Picea* and *Ulmus* pollen also increased, whereas other temperate trees expanded to a lesser extent (*Quercus, Tilia, Fraxinus, Corylus* and *Fagus*). The AP/NAP ratio was very high, around 95%. *Larix* and *Juniperus* pollen almost disappeared together with *Ephedra*. Open-landscape pollen taxa, such as *Artemisia* and Gramineae, remained dominant among the herbs but their abundances decreased along with Chenopodiaceae. Microcharcoal also decreased. In contrast, pollen of *Cannabis/Humulus* t. appeared. The next zone (Hp-3; 915–820 cm, 11,050–9750 cal yr BP) was characterised by the onset of temperate deciduous forests in the landscape. Pollen of *Ulmus* (30–40%) was dominant, pollen of *Quercus* (5–10%), *Fraxinus* (5–10%), *Tilia* (<5%) and *Picea* (5–20%) increased substantially, whereas pollen of *Betula* and *Alnus* decreased. This zone is also characterised by higher abundance of *Picea* stomata indicating the presence of this tree near the lake. The AP/NAP ratio was still high. The zone Hp-4 (815–715 cm; 9700–8900 cal yr BP) was characterised by a distinct decrease of *Ulmus* (from ca 30 to 10%) and steep increase of *Corylus* pollen (up to 50–55%) indicating rather dry climate. Pollen of *Pinus, Picea* and *Betula* decreased, whereas *Acer* and *Fagus* pollen started to increase even if at low abundances. The AP/NAP ratio stabilised around 95%. *Artemisia* and Gramineae reached their lowest values, but their curves remained continual and uninterrupted indicating presence of treeless vegetation somewhere in a wide region, probably at lower altitudes. In the next zone (Hp-5; 710–430 cm; 8850–6250 cal yr BP), *Corylus* decreased slowly (down to 35%), but still remained dominant, whereas *Picea* pollen and stomata increased slightly. *Fagus* and *Acer* pollen curves were already continual (closed curves) and, at the end of the zone, pollen of *Carpinus* also appeared. Microcharcoal influx had decreasing values during this zone. Finally, zone Hp-6 (425–345 cm; 6150–5100 cal yr BP), the last zone of the pollen record in the lake sediments, was characterised by a steep increase in *Fagus* (up to 40%) and *Carpinus* (about 15%) pollen. Pollen of other tree taxa (*Ulmus, Quercus, Tilia, Fraxinus*) decreased slightly (to 5–10%) and pollen of *Corylus* decreased steeply (to 5%). The first pollen grains of *Abies* appeared and AP/NAP remained high.

3.7. Results of geochemical analyses

According to geochemical composition, the profile was divided into six zones (Fig. 8). While the sediments were composed of mainly mineral components in the zone HG-1, autochthonous components like organic matter (represented by LOI) and biogenic silica (Si or Si/Zr in XRF analysis, microscopic observation of diatom frustules) were present in substantial amounts in all other zones. In zone HG-1 there are several cycles of changing input of mineral matter. In the minima of these cycles (minima of lithogenic elements) there are the first maxima of Si/Zr representing the biogenic silica to mineral matter ratio (1010–1005 cm; ca 12.100–12.050 cal yr BP). In the zone HG-2 the Si/Zr ratio is much increased, whereas Zr/Rb and Zr/Ti decreased slightly, which we interpret as fining of mineral grains. The change between zones HG-1 and HG-2 (LG/Early Holocene transition) was very abrupt. From zone HG-1 up to zone HG-4 the element ratios show increasing weathering intensity, K/Ti decreases, while Rb/K increases. In zone HG-3, only 10 cm thick but very distinct, there is a maximum of mineral matter components (increase of all lithogenic elements and MS) at the expense of biogenic silica, with only a minor change in the lithogenic element ratios. This suggests that the nature of the mineral matter did not change much but its input was enhanced, or, alternatively, productivity suddenly dropped. Zone HG-3 is an interruption of the system evolution. Subsequent zone HG-4 is not much different geochemically than zone HG-2. The Si/Zr ratio in zone HG-4 is even higher than in zone HG-2 indicating the highest proportion of the biogenic silica in the sediment. The boundary of zones HG-4/5 is abrupt, the transient strata are only 20 cm thick. Zone HG-5 resembles zone HG-3. The amount of clastics increases at the expense of the biogenic silica with the clastics characterised by enhanced proportion of silt/finest sand content (higher Zr/Rb). Simultaneously MS increases nearly to the level of the prevalently clastic zone HG-1. Zone HG-5 is terminated abruptly by a return to enhanced biogenic silica content at the expense of mineral matter components (beginning of the zone HG-6). Contrarily to the zones HG-2 and HG-4, MS is enhanced in the zone HG-5 and 6, although total Fe content remains more or less the same. Generally, higher MS in zones HG-5 and HG-6 is not proportional to the rather weakly enhanced Zr/Rb ratio. This, together with the nearly constant content of total Fe, suggests that these higher values are probably not related to a higher amount of coarser lithogenic magnetite grains or other magnetic mineral grains. Either large amounts of diamagnetic biogenic opal in underlying zones (high Si/Zr) or post-depositional destruction of magnetic minerals decreased MS in the zones with high productivity.

4. Discussion

4.1. Potential effects of productivity and water table changes on the reconstruction

The T_{July} reconstruction based on chironomids corresponds well with results of other climate proxies in East-Central and Eastern Europe (pollen: Feurdean et al., 2008a,b; chironomids: Tóth et al., 2012, 2015; Płóciennik et al., 2011; stalagmites: Tamaş and Causse, 2001, Demény et al., 2013). It was recently illustrated that co-varying factors in calibration datasets may influence reconstructions based on biotic proxy-indicators (Velle et al., 2010;

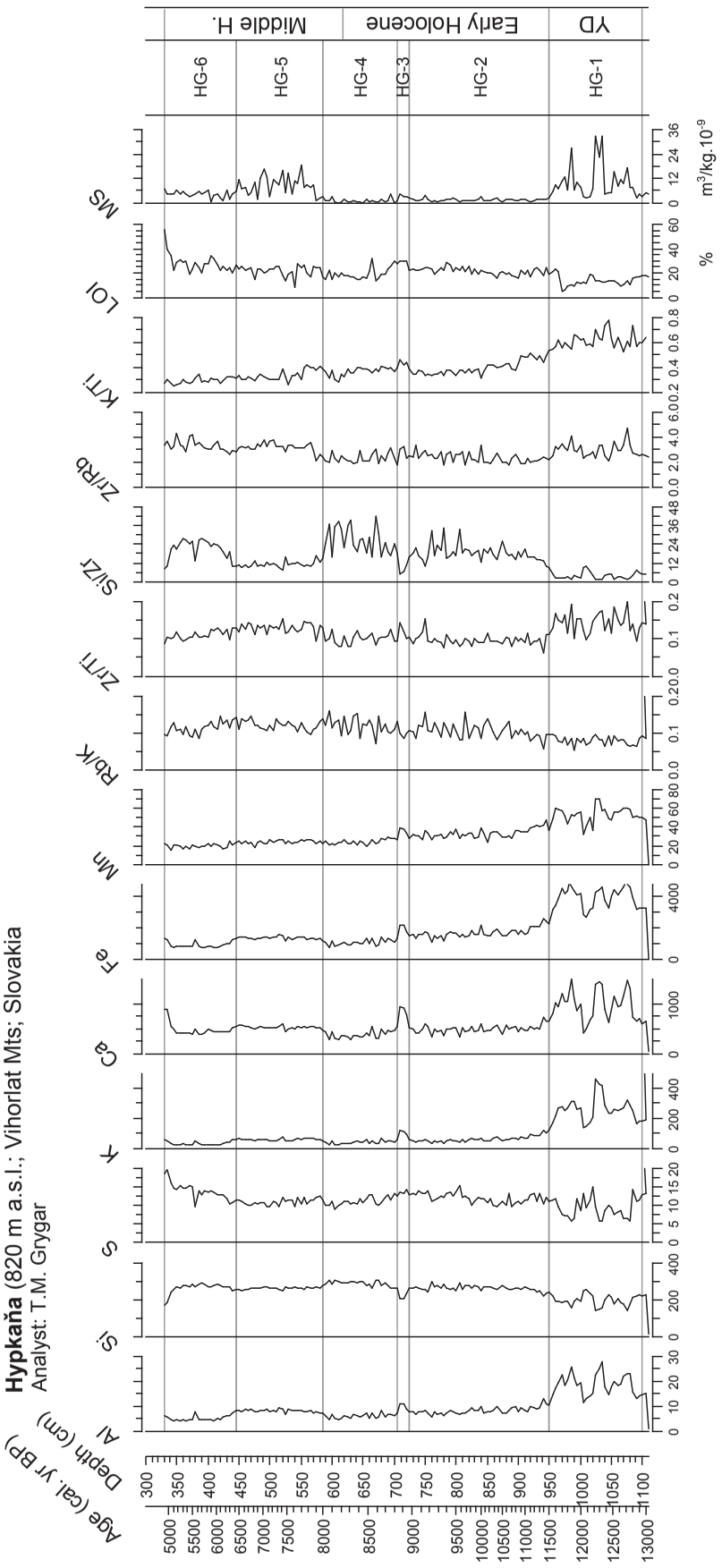

Fig. 8. Results of geochemical analyses, magnetic susceptibility (MS) and loss-on-ignition (LOI at 550 °C). Also ratios of some elements are shown.

Juggins, 2013). In the case of reconstructions based on chironomids, Brodersen and Anderson (2002) demonstrated that taxa with high temperature optima occur mostly in eutrophic conditions and taxa with low temperature optima occur in oligotrophic conditions. This positive correlation between temperature and trophic status was documented to some extent in most of the published calibration datasets (Brooks and Birks, 2001; Heiri and Lotter, 2005; Heiri et al., 2011). If these two environmental factors develop independently, the T_{July} reconstructions may be biased. Therefore we reconstructed trophic status using diatom-inferred TP to assess whether past variations in TP may have led to potential problems in the T_{July} reconstruction. Diatom-inferred TP stayed relatively constant in the profile varying between 23 μg L^{-1} (in 955 cm, 11.500 cal yr BP) and 80 μg L^{-1} (in 700 cm, 8800 cal yr BP). However, an increase (from 39 μg L^{-1} to 79 μg L^{-1}) is registered at 8850 cal yr BP (from 710 cm up), with fluctuating values and only few short-term decreases thereafter (most distinct in 640–630 cm; 8300–8400 cal yr BP). In contrast, chironomid-inferred T_{July} decreased at 8700 cal yr BP and with the exception of 7600–7700 cal yr BP stayed lower than in the Early Holocene (Fig. 3). As the relationship between temperature and trophic status in this part of the profile is negative, not positive, we exclude a bias in T_{July} reconstruction caused by a positive interaction. Further, also minimum values during the YD (at ca 12,000 and 12,500 cal yr BP) were characterised by moderate increases in diatom-inferred TP (Fig. 3).

Another factor, which might influence T_{July} reconstruction is the changing depth of the lake as water in the shallow lake can be strongly warmed during the summer, whereas deep stratified lakes are characterised by profundal environments with optimal conditions for cold-demanding chironomid taxa (Velle et al., 2010). A deepening of the lake could therefore, in principle lead to a decrease in reconstructed Holocene temperatures. However, the most pronounced decrease in the Holocene part of the record at 8700 cal yr BP was probably associated with a decrease of the lake depth probably due to terrestrialization, as suggested by a decrease in planktonic diatoms and algae and by high abundance of *Aulacoseira* species (Saunders et al., 2008). An opposite situation was observed within the YD period. Here, higher reconstructed T_{July} values are related to the lower inferred lake depth (Fig. 3). Thus in this section of the record the reconstructed T_{July} values could be slightly biased (increased) by lake level variations, although they still remained in the range of the YD temperatures and were clearly cooler than reconstructed Holocene temperatures. Finally, the reconstructed increase of T_{July} after 7000 cal yr BP could be called into question, because the lake started to terrestrialize up to ca 5000 cal yr BP, when the open water surface completely disappeared and thus the depth of lake was decreasing.

4.2. Younger Dryas T_{July} fluctuations and the LG/Holocene transition

Focusing on the reconstructed T_{July} for the YD, we recorded very variable temperatures between 7.2 and 10.8 °C at 820 m a.s.l. (i.e. ca 12.1–15.7 °C adjusted to modern sea level, ca 49°N). These values are considerably lower (about ca 4.5 °C) than those reconstructed at more southerly locations in the eastern and central parts of Southern Europe (42–44.5°N) or the Alpine region (ca 46°N), but about 3 °C higher than in the Baltic region (56.5–58°N) or British Isles (54–55.5°N) situated more to the north (Heiri et al., 2014a). It seems that reconstructed values reflect the latitude, because reconstructed T_{July} is intermediate. As the study site is geographically closer to the Alps than to the Baltic region, the reconstructed values are likely slightly lower then would be expected according to latitude, which might be attributed to the exposition of the study site (northern slopes). The comparison with the record from central Poland (almost 52°N, 13–16 °C corrected to 0 m a.s.l.; Płóciennik et al., 2011) also suggests slightly lower T_{July} values at our study site than would be expected according to latitude. The rather distinct climatic fluctuations during the YD resemble minor variations recorded in the oxygen isotope records of the Greenland ice sheet (e.g. Lowe et al., 2008; Rasmussen et al., 2014) and also by other non-quantitative climate proxies in Europe (Von Grafenstein et al., 1999). However, Younger Dryas summer temperatures reconstructed in other chironomid records (e.g. Tóth et al., 2012; Ilyashuk et al., 2009; Brooks and Birks, 2001) are much more stable and other YD reconstructions from Europe also do not show such minor centennial-scale oscillations (e.g. Lauterbach et al., 2011).

Some previous studies have suggested that YD climate was unstable. For example, it has been proposed that rapid alternations between glacial growth and melting may have affected sea-ice cover and the influx of warm salty water in the Nordic sea (Bakke et al., 2009). Schwark et al. (2002) suggested a middle Younger Dryas warming (MYDE; 12,200–12,300 cal yr BP) in southwestern Germany by increased pollen productivity of *Betula* and increased content of nC_{27}-alkanes in the lake sediment which correspond with increased input of *Betula* litter to the lake. Such short-term warmings are also apparent in the NGRIP and GRIP ice core data (Rasmussen et al., 2014), which show several short positive excursions of $\delta^{18}O$, although the amplitude of these changes is small compared with the centennial scale shifts between the YD and adjacent climate periods. High YD fluctuations were recorded also in the Eastern Carpathians by means of variability in ^{18}O content in stalagmites (Tamaş and Causse, 2001). Sediment composition from the YD period also varied considerably in our record, confirming that local environmental conditions were affected by climatic changes at our study site (Fig. 8). In the chironomid-inferred T_{July} record, there are two warmer periods dated to 12,850–12,600 cal yr BP and, more distinctly, at 12,400–12,200 cal yr BP within the YD. These warmer phases coincide with distinct water level declines which are indicated in our record by gradual displacement of aquatic taxa by terrestrial ones and by changing input of mineral matter into the lake (Fig. 8). Low lake level episodes have been recorded also in Central Europe during the YD and were accompanied by changes in sediment composition as well (cf. Karasiewicz et al., 2013). Since temperature variations inferred by chironomids within the YD co-vary with apparent changes in water table, this may have influenced the results. Furthermore, inferred temperature variations within the YD are within the prediction error of the age-depth model (Fig. 3). We conclude that our results suggest that July air temperatures may have shown centennial-scale variations at the study site, but that these changes coincided, and may have been amplified, by local hydrological changes. Additional evidence (e.g. additional YD temperature reconstructions for the study region) will have to be developed to resolve whether these variations represent real air temperature changes or chironomid response to other environmental variations (e.g. changes in water table).

The LG/Holocene transition was characterised by a rapid increase of the reconstructed T_{July}. The beginning of the warming in our record is dated to between ca. 11,700 and 11,600 cal yr BP (from 10.3 to 13.7 °C), which agrees with the onset of Holocene assessed as Global Stratotype section in NGRIP (11,700 b2k, Walker et al., 2009). In the next sample temperatures rise by another 1.8 °C (from 13.7 to 15.5 °C) to reach a first maximum at ca 11,400 cal yr BP. Thus in ca. 300 years the T_{July} has apparently increased by ca. 5 °C. According to the review of Heiri et al. (2014a), a similar steep increase of reconstructed T_{July} has been recorded in some sites in Alpine region (by ca 4 °C) but especially also at higher latitudes (British islands by ca 5 °C, Norway 4–5 °C). Much lower and slower warming occurred at low latitudes (SW Europe, E and CS Europe) and altitudes (Baltic region, Heiri et al., 2014a; almost no change in

Holocene onset in middle Poland, Płóciennik et al., 2011). The only chironomid-based T_{July} reconstruction from the whole Carpathians (45°N, Retezat Mts; Tóth et al., 2012) has also shown a delayed warming at the beginning of the Holocene by about 2.5–3 °C. At the YD to Holocene transition no major changes in summer temperature was detected in this record, but summer temperatures then increased in two steps and reached 12.0–13.3 °C during the Preboreal. The comparison of pollen data from the Western Carpathians and the adjacent areas indicates that during the LG the pollen spectrum of the study site was similar to the sites located in steppe-tundra landscapes of the Inner-Carpathian basins (e.g., Hájková et al., 2015), while just after the Holocene onset it became similar to samples from Western Slovakia which are rich in temperate trees (Petr et al., 2013; Hájková et al., 2013). Such a conspicuous development towards a temperate landscape is exceptional within East-Central Europe as is indicated also by gradient analysis of available pollen samples from the LG and Holocene onset (Jamrichová et al. unpublished data) and might be caused by the geographic position of the study site on the boundary between oceanic and continental climate influences. The LG/Holocene transition was apparently accompanied by a steep increase of lake depth indicated by increased representation of planktonic diatoms and algae (*Tetraedron minimum*), by a decrease of coarse-clastic input to the lake sediment and a steep decline of magnetic susceptibility. These changes could be attributed to the climate moistening which followed climate warming (e.g. Feurdean et al., 2008a). This climate improvement triggered rapid spread of deciduous trees, firstly *Betula*, which has probably spread into the semi-open forest-tundra above the lake, then *Alnus,* which has occupied wet places near the lake and forest springs (ca 11,600 cal yr BP) and later also *Ulmus* (11,300–11,000 cal yr BP). The rapid reaction of *Betula* to climate improvement was recorded also by macrofossils in the Eastern Carpathians (at ca 11,500 cal yr BP; Feurdean et al., 2008b) and by pollen and lipid biomarkers in Central Europe (Schwark et al., 2002).

4.3. Holocene thermal maximum

Another often studied and discussed topic is the timing and duration of the Holocene thermal maximum (HTM) in summer temperature, which is mostly positioned in the large interval of 11 and 5 ka BP (Renssen et al., 2009, 2012). Based on global atmosphere-ocean-vegetation model runs, Renssen et al. (2012) have revealed that in large sections of Europe the timing of HTM is expected to be between 7 and 6 ka BP, which agrees with some proxy-based reconstructions (e.g. Heiri et al., 2014b; Renssen et al., 2009). For example, based on pollen assemblages Davis et al. (2003) reconstructed maximum summer temperatures around 6 ka for Northern Europe and Western Central Europe and around 7–8 ka in central eastern Europe. However, reconstruction based on other proxy records placed the HTM to different sections of this interval, some of them also to the Early Holocene (9500–9100 cal yr BP (Tóth et al., 2015) or 10,000–8600 cal yr BP (Ilyashuk et al., 2011)). In our study site, the sample with the highest reconstructed T_{July} was at the beginning of the Holocene (15.5 °C at 11,400 cal yr BP and 15.0 °C at 10,750 cal yr BP), but the whole period 11,600–8850 cal yr BP was relatively warm with temperatures being slightly higher, the same or slightly lower than today (13.7–15.5 °C; today temperature for the altitude of the lake estimated to 14.7 °C). Temperature was slowly decreasing from ca. 10,500 cal yr BP onwards toward the Early/Middle Holocene transition with an exception of short cooling event at about 11,200 cal yr BP (11.9 °C). A possible reason for the discrepancy between the different records is that local orography and the effects of mountain ranges may have influenced local climates, leading to earlier Holocene temperature maxima in regions which are downwind from mountain ranges and, e.g., shielded from the influence of North Atlantic air masses. In these situations the high summer insolation values of the Early Holocene may have led to higher temperatures than later in the Holocene period. Alternatively, changes in water tables discussed above may have to some extent affected chironomid assemblages and influenced the trend in chironomid-inferred temperatures. However, since an early HTM has also been reported from other Holocene records from European mountain lakes, we consider orographic effects or regional differences in the timing of the HTM across Europe the more likely explanation.

4.4. Early/Middle Holocene cooling

We recorded a distinct T_{July} decrease (from 13.9 to 10.1 °C) between 8850 and 8750 cal yr BP, which lasted to ca 8000 cal yr BP (Fig. 3). A distinct cooling event at 8200 yr BP lasting for 100–200 years has been reported from the Greenland ice core oxygen isotope records but also many other climate records from around the North Atlantic (Alley and Ágústsdóttir, 2005). Mayewski et al. (2004) showed that this cooling event was embedded, or formed part of, a longer lasting period of climate variations they named the first Holocene rapid climate change (RCC) placed to 9000–8000 cal yr BP. Short lived cooling events within this period have been reported from several other chironomid records. Heiri et al. (2003) described a period of cooler summer temperatures (ca. 8200–7800 cal yr BP) which coincided with changing meltwater flux from the American continent to the North Atlantic (Heiri et al., 2004). A decrease of chironomid-inferred T_{July} was also recorded in the central Poland (Płóciennik et al., 2011: 8700–8000 cal yr BP) and from the eastern central Alps (Ilyashuk et al., 2011: 8200–8000 cal yr BP). A temperature decrease was also recorded by oxygen isotope composition of diatoms in the Eastern Carpathians (Magyari et al., 2013) and by oxygen isotope data from a Hungarian speleothem (Demény et al., 2013: 9000–8000 yr BP). Based on pollen-inferred temperatures, Feurdean et al. (2008a) detected a decrease of winter temperatures (in the coldest month) between 8200 and 8000 cal yr BP, whereas summer temperatures did not change. Total pollen influx in our record (mostly of *Ulmus, Quercus, Fraxinus* and *Corylus*; data not shown) decreased at ca 8700 cal yr BP probably due to decreased pollen productivity as a reaction to climate deterioration (Fig. 7, Andersen, 1980; Sjögren et al., 2006). At the study site, simultaneously other analysed parameters and proxies also changed at about 8700 yr BP. The duration of the cold episode at 8700–8000 cal yr BP is distinctly longer in our record than reported for the 8.2 ka event (e.g. Wiersma and Renssen, 2006). However, since we have only a limited number of radiocarbon dates in this section of the record (Fig. 2, Table 1) we cannot rule out that this event is shorter than dated in our records. Alternatively, the cooling could be related to the longer first Holocene RCC described by Mayewski et al. (2004).

Geochemical analyses have shown that the cool period in our core came after an abrupt short-term input of mineral matter into the lake indicated by an increase of all lithogenic elements and MS and decrease of biogenic silica proxy (cf. zone HG-3, Fig. 8), which was reflected by dominance of tychoplanktonic diatoms in the sediment (Fig. 6). Both proxies could indicate increased precipitation resulting in higher erosion and more intense water column mixing in the lake, such as due to enhanced wind. Enhanced mixing usually creates an upward flux of nutrients and silica from the hypolimnion (Stone et al., 2011), which would agree with increased diatom-inferred TP in our record. Also increased *Alnus* pollen (both percentages and influx) might indicate higher wetness and

development of wet alder carr in the terrestrialized littoral or expanding wetlands in the surrounding landscape. Moreover, *Alnus* was revealed to have higher pollen productivity under wetter climate in the research of pollen traps (Van der Knaap et al., 2010). The climate moistening in this period (8700–8600 cal yr BP) is also documented by a conspicuous expansion of temperate forests in our record (decline of *Corylus*, slight increase of *Ulmus*, *Fagus* and *Picea*) and also in other records from the deciduous-forest zone of the Carpathians (Feurdean et al., 2015; Hájek et al., 2016). Increased precipitation in Central and East-Central Europe was reconstructed also by testate amoebae (higher water level at 8300–8000 cal yr BP, Schnitchen et al., 2006), by increased water level of lakes (8300–8000 and 7500–7000 cal yr BP, Magny, 2004; 8400 cal yr BP, Buczkó et al., 2013) or climate-mediated decline of fire activity expressed by decrease of charcoal influx at about 8500 cal yr BP (Feurdean et al., 2012, 2015). Even if the timing in these records is not completely the same as in our study, the differences are not so high to clearly exclude synchronicity and might be caused by some inaccuracy in age-depth models. Nevertheless, the timing of climate moistening could be also affected by local and regional factors like position on mountain ranges, distance from the Atlantic or prevailing wind direction. According to Magny et al. (2003), mid-latitudes between ca 50° and 43° responded to the cooling by wetter climate, whereas Southern and Northern Europe had contrarily drier climate. The extent of this wet mid-European zone could reflect the strength of the Atlantic Westerly Jet in relation to the thermal gradient between low and high latitudes (Magny et al., 2003). Moreover, climate moistening was probably associated with increased cloudiness, which could have prevented warming of the lake water in summer and thus locally amplified the effect of cooling and decreased values of reconstructed T_{July}.

It is remarkable that indicators of erosion and turbulent water conditions were present only before the reconstructed cold period and later no input of eroded inorganic matter from the surrounding landscape to the lake was detected by geochemical analyses (Fig. 8). Likely the development of terrestrial vegetation in the lake surrounding triggered by climate moistening prevented further erosion, as suggested by increase of tree pollen (*Tilia, Fagus, Picea*) and decrease of *Corylus* pollen. This period is also characterised by increased diatom-inferred total phosphorus content (Fig. 3). Increased trophic state and nutrient availability for autotrophic organisms in the lake is indicated also by increased abundance of nutrient-demanding algae *Pediastrum boryanum* agg. (Fig. 6). There are several possible mechanisms of nutrient enrichment of lake water. It could have been caused by increased input of litter from nearby trees, especially *Alnus*. Another explanation could be flux of nutrients from the hypolimnion due to enhanced wind activity (e.g. Stone et al., 2011). Input of phosphorus through the erosion from the surrounding catchment may have been possible only at the beginning of the cold phase, later such an increased nutrient input is not supported by geochemical analyses, as the proxies for clastic input (Zr/Rb, Zr/Ti or Rb/K) did not change. Another possible mechanism for changes in nutrient availability in the lake could have been changes in seasonality connected with cooling of climate. The prolonged winters could have caused longer ice cover and thus stronger stratification in the lake, anoxia in the hypolimnion and consequent internal phosphorus loading (Kirilova et al., 2009). Released phosphorus would then become available for organisms after spring mixing of hypo- and epilimnetic layers. However, increased phosphorus concentrations were not so distinctly reflected in the species composition of chironomids since the proportion of eutrophic and oligotrophic taxa was rather equal in this zone (Fig. 6) and oligotrophic taxa distinctly increased their abundances compared to the previous zone. It was documented that the reaction of heterotrophic chironomids to changes in lake water nutrients is not as predictable as the reaction of autotrophic organisms because chironomids are influenced by increased productivity indirectly through the food availability (macrophytes, algae, but also other invertebrates and organic detritus) and oxygen concentrations (Brodersen and Lindegaard, 1999; Brodersen and Quinlan, 2006), which could be influenced also by other factors than phosphorus availability. Moreover, fossil chironomid records from the central part of small lakes are composed by species from both, the littoral and the profundal, where different environmental conditions can occur (Van Hardenbroek et al., 2011). Jeppesen et al. (1997) demonstrated that littoral environments can host more oligotrophic taxa than the profundal and their input to deepest part of lakes can shift the chironomid signal to more oligotrophic conditions. Also oxygen availability in the profundal might be an important factor. If for some reasons (e.g. cold climatic conditions) the oxygen amount remains high in the profundal, the chironomid species composition may stay the same (cold-demanding oligotrophic taxa) and may not react on the increased nutrient input (Brooks and Birks, 2001; Little et al., 2000).

5. Conclusions

From the analysis of an almost 7 m thick layer of lake sediments from East-Central Europe (Carpathian Mts.), we inferred considerable variation in environmental conditions and in particularly mean July temperatures reconstructed from chironomids during the latest Glacial and Early Holocene. In the cold YD, T_{July} was on average around 9.5 °C with lowest values about 7 °C. Considerable temperature variability within the YD was inferred, with two warmer events (12,850–12,600 and 12,200–12,400 cal yr BP) which may have been related to instability of climate recorded in other records (e.g. the Nordic Seas). Other chironomid records from Europe typically do not feature within YD temperature variability of this amplitude. However other proxies (geochemistry, diatoms) support climatic variations, particularly hydrological changes, at the study site during this interval and suggest that warmer conditions were accompanied by a water table decrease. The YD was followed by distinct warming of up to 5 °C between 11,600–11,400 cal yr BP. The warmest Holocene temperatures (15–15.5 °C) were recorded in the earlier part of the Holocene between 11,400 and 8850 cal yr BP. This agrees with some other chironomid records from European mountain ranges (Carpathians, central Alps) but contrasts with other reconstructions from different parts of Europe. Possibly this difference is related to local topographic effects on local climates or regional differences in Holocene climate development within Europe. During the course of the Holocene, a distinct but short-lived cooling was reconstructed around 11,200 cal yr BP, possibly corresponding with the 11.4 ka event and a more pronounced cooling event between 8700 and 8000 cal yr BP. The timing of the latter cooling coincides with cool episodes recorded in other palaeoclimate records from Europe and the North Atlantic region. The cooling is longer than reported for the 8.2 ka event, but similar in duration as the longer lasting cooling episode referred to as the first Holocene RCC by Mayewski et al. (2004) that the 8.2 ka event is embedded in. At Hypkaňa geochemical evidence and the composition of diatom assemblage supported a shift to wet and cold conditions during this interval.

Author contributions

PH and LP conceived the research, LP identified pollen and green algae, prepared samples for geochemical analyses and measured LOI and MS, PP identified chironomids and prepared data for quantitative reconstruction of T_{July}, BCh identified diatoms and prepared data for quantitative reconstruction of TP and TMG

carried out geochemical analyses. PH created age-depth model and prepared samples for AMS dating. OH calculated chironomid-inferred T_{July}. All authors provided ecological interpretations of results and participated on the preparing of manuscript, which was leaded by PH.

Acknowledgement

The research was financed by the grant project of the Czech Science Foundation (P504/11/0429), by institutional supports and project MUNI/A/1048/2015 of Masaryk University and Czech Academy of Sciences (RVO 67985939). We are grateful to Ondřej Hájek for creating the map, our colleges M. Hájek, L. Dudová, T. Duda and S. Rezník for help by coring the profile in the field and anonymous reviewer for valuable comments. E. Jamrichová helped us with preparing of pollen diagram.

Appendix A. Supplementary data

Supplementary data related to this article can be found at http://dx.doi.org/10.1016/j.quascirev.2016.04.001.

References

Alley, R.B., Ágústsdóttir, A.M., 2005. The 8k event: cause and consequences of a major Holocene abrupt climate change. Quat. Sci. Rev. 24, 1123–1149.
Andersen, S.T., 1980. Influence of climatic variation on pollen season severity in wind-pollinated trees and herbs. Grana 19, 47–52.
Bakke, J., Lie, Ø., Heegaard, E., Dokken, T., Haug, G.H., Birks, H.H., Dulski, P., Nilsen, T., 2009. Rapid oceanic and atmospheric changes during the Younger Dryas cold period. Nat. Geosci. 2, 202–205.
Battarbee, R.W., Jones, V.J., Flower, R.J., Cameron, N.G., Bennion, H., Carvalho, L., Juggins, S., 2001. Diatoms (Pp. 155–202. Springer, Netherlands.
Beug, H.J., 2004. Leitfaden der Pollenbestimmung: für Mitteleuropa und angrenzende Gebiete. Pfeil, München.
Blockley, S.P.E., Lane, C.S., Hardiman, M., Rasmussen, S.O., Seierstand, I.K., Steffensen, J.P., et al., 2012. Synchronization of palaeoenvironmental records over the last 60,000 years, and an extended INTIMATE event stratigraphy to 48,000 b2k. Quat. Sci. Rev. 36, 2–10.
Bouchez, J., Gaillardet, J., France-Lanord, C., Maurice, L., Dutra-Maia, P., 2011. Grain size control of river suspended sediment geochemistry: clues from Amazon River depth profiles. Geochem. Geophys. Geosyst. 12 (3), 1–24.
Brodersen, K.P., Anderson, N.J., 2002. Distribution of chironomids (Diptera) in low arctic West Greenland lakes: trophic conditions, temperature and environmental reconstruction. Freshw. Biol. 47, 1137–1157.
Brodersen, K.P., Lindegaard, C., 1999. Classification, assessment and trophic reconstruction of Danish lakes using chironomids. Freshw. Biol. 42, 143–157.
Brodersen, K.P., Quinlan, R., 2006. Midges as paleoindicators of lake productivity, eutrophication and hypolimnetic oxygen. Quat. Sci. Rev. 25, 1995–2012.
Bronk Ramsey, C., 2009. Bayesian analysis of radiocarbon dates. Radiocarbon 51, 337–360.
Brooks, S.J., Birks, H.J.B., 2001. Chironomid-inferred air temperatures from lateglacial and Holocene sites in north-west Europe: progress and problems. Quat. Sci. Rev. 20, 1723–1741.
Brooks, S.J., Langdon, P.G., Heiri, O., 2007. The Identification and Use of Palaearctic Chironomidae Larvae in Palaeoecology. QRA Technical Guide No. 10. Quaternary Research Association, London.
Buczkó, K., Magyari, E.K., Braun, M., Bálint, M., 2013. Diatom-inferred lateglacial and Holocene climatic variability in the south Carpathian mountains (Romania). Quat. Int. 271, 123–135.
Clark, P.U., Marshall, S.J., Clarke, G.K.C., Hostetler, S.W., Licciardi, J.M., Teller, J.T., 2001. Freshwater forcing of abrupt climate change during the last glaciation. Science 293 (5528), 283–287.
Davis, B.A.S., Brewer, S., Stevenson, A.C., Guiot, J., Contributors, D., 2003. The temperature of Europe during the Holocene reconstructed from pollen data. Quat. Sci. Rev. 22, 1701–1716.
Demény, A., Czuppon, G., Siklósy, Z., Leél-Őssy, S., Lin, K., Shen, C.C., et al., 2013. Mid-Holocene climate conditions and moisture source variations based on stable H, C and O isotope compositions of speleothems in Hungary. Quat. Int. 293, 150–156.
Dudová, L., Hájková, P., Opravilová, V., Hájek, M., 2014. Holocene history and environmental reconstruction of a Hercynian mire and surrounding mountain landscape based on multiple proxies. Quat. Res. 82, 107–120.
Faegri, K., Iversen, J., 1989. Textbook of Pollen Analysis, fourth ed. Wiley, Chichester, p. 328.
Feurdean, A., Klotz, S., Mosbrugger, V., Wohlfahrt, B., 2008a. Pollen-based quantitative reconstructions of Holocene climate variability in NW Romania. Palaeogeogr. Palaeoclimatol. Palaeoecol. 260, 494–504.
Feurdean, A., Klotz, S., Brewer, S., Mosbrugger, V., Tămaş, T., Wohlfarth, B., 2008b. Lateglacial climate development in NW Romania – comparative results from three quantitative pollen-based methods. Palaeogeogr. Palaeoclimatol. Palaeoecol. 265, 121–133.
Feurdean, A., Spessa, A., Magyari, E., Willis, K.J., Veres, D., Hickler, T., 2012. Trends in biomass burning in the Carpathian region over the last 15,000 years. Quat. Sci. Rev. 45, 111–125.
Feurdean, A., Perşoiu, T., Stevens, S., Magyari, E.K., Onac, B.P., Markovič, S., et al., 2014. Climate variability and associated vegetation response throughout Central and Eastern Europe (CEE) between 60 and 8 ka. Quat. Sci. Rev. 106, 206–224.
Feurdean, A., Marinova, E., Nielsen, A.B., Liakka, J., Veres, D., Hutchinson, S.M., et al., 2015. Origin of the forest steppe and exceptional grassland diversity in Transylvania (central-eastern Europe). J. Biogeogr. 42, 951–963.
Grimm, E.C., 2011. TGView Version 1.5.12. Illinois State Museum, Research and Collections Center, Springfield.
Grygar, T., Světlík, I., Lisá, L., Koptíková, L., Bajer, A., Wray, D.S., et al., 2010. Geochemical tools for the stratigraphic correlation of floodplain deposits of the Morava River in Strážnické Pomoraví, Czech Republic from the last millennium. Catena 80 (2), 106–121.
Hájek, M., Dudová, L., Hájková, P., Roleček, J., Moutelíková, J., Jamrichová, E., et al., 2016. Contrasting Holocene environmental histories may explain patterns of species richness and rarity in a Central European landscape. Quat. Sci. Rev. 133, 48–61.
Hájková, P., Jamrichová, E., Horsák, M., Hájek, M., 2013. Holocene history of a *Cladium mariscus*-dominated calcareous fen in Slovakia: vegetation stability and landscape development. Preslia 85, 289–315.
Hájková, P., Horsák, M., Hájek, M., Jankovská, V., Jamrichová, E., Moutelíková, J., 2015. Using multi-proxy palaeoecology to test a relict status of refugial populations of calcareous-fen species in the Western Carpathians. Holocene 25, 702–715.
Heiri, O., Lotter, A.F., 2001. Effect of low count sums on quantitative environmental reconstructions: an example using subfossil chironomids. J. Paleolimnol. 26, 343–350.
Heiri, O., Lotter, A.F., 2005. Holocene and Lateglacial summer temperature reconstruction in the Swiss Alps based on fossil assemblages of aquatic organisms: a review. Boreas 34, 506–516.
Heiri, O., Lotter, A.F., 2010. How does taxonomic resolution affect chironomid-based temperature reconstruction? J. Paleolimnol. 44, 589–601.
Heiri, O., Lotter, A.F., Lemcke, G., 2001. Loss on ignition as a method for estimating organic and carbonate content in sediments: reproducibility and comparability of results. J. Paleolimnol. 25, 101–110.
Heiri, O., Lotter, A.F., Hausmann, S., Kienast, F., 2003. A chironomid-based Holocene summer air temperature reconstruction from the Swiss Alps. Holocene 13, 477–484.
Heiri, O., Tinner, W., Lotter, A.F., 2004. Evidence for cooler European summers during periods of changing meltwater flux to the North Atlantic. PNAS 101 (43), 15285–15288.
Heiri, O., Brooks, S.J., Birks, H.J.B., Lotter, A.F., 2011. A 274-lake calibration data-set and inference model for chironomid-based summer air temperature reconstruction in Europe. Quat. Sci. Rev. 30, 3445–3456.
Heiri, O., Brooks, S.J., Renssen, H., Bedford, A., Hazekamp, M., Ilyashuk, B., et al., 2014a. Validation of climate model-inferred regional temperature change for late-glacial Europe. Nat. Commun. 5, 4914.
Heiri, O., Koinig, K.A., Spötl, C., Barrett, S., Brauer, A., Drescher-Schneider, R., et al., 2014b. Palaeoclimate records 60-8 ka in the Austrian and Swiss Alps and their forelands. Quat. Sci. Rev. 106, 186–205.
Holliday, V.T., 2004. Soils in Archaeological Research. Oxford University Press, Oxford.
Holmes, N., Langdon, P.G., Caseldine, C., Brooks, S.J., Birks, H.J.B., 2011. Merging chironomid training sets: implications for palaeoclimate reconstructions. Quat. Sci. Rev. 30, 2793–2804.
Hošek, J., Pokorný, P., Kubovčík, V., Horáček, I., Žáčková, P., Kadlec, J., et al., 2014. Late glacial climatic and environmental changes in eastern-central Europe: correlation of multiple biotic and abiotic proxies from the Lake Švarcenberg, Czech Republic. Palaeogeogr. Palaeoclimatol. Palaeoecol. 396, 155–172.
Hu, Z.-C., Gao, S., 2008. Upper crust abundances of trace elements: a revision and update. Chem. Geol. 253, 205–221.
Ilyashuk, B., Gobet, E., Heiri, O., Lotter, A.F., van Leeuwen, J.F.N., van der Knaap, W.O., et al., 2009. Lateglacial environmental and climatic changes at the Maloja Pass, Central Swiss Alps, as recorded by chironomids and pollen. Quat. Sci. Rev. 28, 1340–1353.
Ilyashuk, E.A., Koinig, K.A., Heiri, O., Ilyashuk, B.P., Psenner, R., 2011. Holocene temperature variations at a high-altitude site in the Eastern Alps: a chironomid record from Schwarzsee ob Sölden, Austria. Quat. Sci. Rev. 30, 176–191.
Jeppesen, E., Jensen, J.P., Søndergaard, M., Lauridsen, T., Pedersen, L.J., Jensen, L., 1997. Top-down control in freshwater lakes: the role of nutrient state, submerged macrophytes and water depth. Hydrobiologia 342/343, 151–164.
Jones, A.F., Macklin, M.G., Brewer, P.A., 2012. A geochemical record of flooding on the upper River Severn, UK, during the last 3750 years. Geomorphology 179, 89–105.
Juggins, S., 2001. The European Diatom Database, User Guide,Version 1.0. http://craticula.ncl.ac.uk/Eddi/docs/EddiGuide.pdf.
Juggins, S., 2007. C2 Version 1.5 User Guide. Software for Ecological and

Palaeoecological Data Analysis and Visualisation. University of Newcastle, Newcastle upon Tyne, UK.
Juggins, S., 2013. Quantitative reconstructions in palaeolimnology: new paradigm or sick science? Quat. Sci. Rev. 64, 20–32.
Karasiewicz, M.T., Hulisz, P., Noryśkiewicz, A.M., Krześlak, I., Świtoniak, M., 2013. The record of hydroclimatic changes in the sediments of a kettle-hole in a young glacial landscape (north-centralPoland). Quat. Int. 328–329, 264–276.
Kirilova, E., Heiri, O., Enters, D., Cremer, H., Lotter, A.F., Zolitschka, B., Hübener, T., 2009. Climate-induced changes in the trophic status of a Central European lake. J. Limnol. 68 (1), 71–82.
Komárek, J., Jankovská, V., 2001. Review of the green algal genus *Pediastrum*; implication for pollen-analytical research. Bibl. Phycol. 108, 1–127.
Laskar, J., Robutel, P., Joutel, F., Gastineau, M., Correia, A.C.M., Levrard, B., 2004. A long term numerical solution for the insolation quantities of the Earth. Astron. Astrophy. 428, 261–285.
Lauterbach, S., Brauer, A., Andersen, N., Danielopol, D.L., Dulski, P., Hüls, M., et al., 2011. Environmental responses to Lateglacial climatic fluctuations recorded in the sediments of pre-Alpine Lake Mondsee (northeastern Alps). J. Quat. Sci. 26 (3), 253–267.
Little, J.L., Hall, R.I., Quinlan, R., Smol, J.P., 2000. Past trophic status and hypolimnetic anoxia during eutrophication and remediation of Gravenhurst Bay, Ontario: comparison of diatoms, chironomids, and historical records. Can. J. Fish. Aquat. Sci. 57, 333–341.
Lowe, J.J., Rasmussen, S.O., Björck, S., Hoek, W.Z., Steffensen, J.P., Walker, M.J.C., Yu, Z.C., Grp, I., 2008. Synchronisation of palaeoenvironmental events in the North Atlantic region during the Last Termination: a revised protocol recommended by the INTIMATE group. Quat. Sci. Rev. 27 (1–2), 6–17.
Magny, M., 2004. Holocene climate variability as reflected by mid-European lake-level fluctuations and its probable impact on prehistoric human settlements. The record of human/climate interaction in lake sediments. Quat. Int. 113 (1), 65–79.
Magny, M., Bégeot, C., Guiot, J., Peyron, O., 2003. Contrasting patterns of hydrological changes in Europe in response to Holocene climate cooling phases. Quat. Sci. Rev. 22, 1589–1596.
Magyari, E., Demény, A., Buczkó, K., Kern, Z., Vennemann, T., Fórizs, I., et al., 2013. A 13,600-year diatom oxygen isotope record from the South Carpathians (Romania): reflection of winter conditions and possible links with North Atlantic circulation changes. Quat. Int. 293, 136–149.
Matys Grygar, T., Elznicová, J., Bábek, O., Hošek, M., Engel, Z., Kiss, T., 2014. Obtaining isochrones from pollution signals in a fluvial sediment record: a case study in a uranium-polluted floodplain of the Ploučnice River, Czech Republic. Appl. Geochem. 48, 1–15.
Mauri, A., Davis, B.A.S., Collins, P.M., Kaplan, J.O., 2015. The climate of Europe during the Holocene: a gridded pollen-based reconstruction and its multi-proxy evaluation. Quat. Sci. Rev. 112, 109–127.
Mayewski, P.A., Rohling, E.E., Stager, J.C., Karlén, W., Maasch, K.A., Meeker, L.D., et al., 2004. Holocene climate variability. Quat. Res. 62, 243–255.
Menviel, L., Timmermann, A., Timm, O., Mouchet, A., 2011. Deconstructing the last Glacial Termination: the role of millennial and orbital-scale forcings. Quat. Sci. Rev. 30 (9), 1155–1172.
Nazarova, L., Herzschuh, U., Wetterich, S., Kumke, T., Petryakova, L., 2011. Chironomid-based inference models for estimating mean July air temperature and water depth from lakes in Yakutia, northeastern Russia. J. Paleolimnol. 45, 57–71.
Petr, L., Žáčková, P., Grygar, T.M., Píšková, A., Křížek, M., Treml, V., 2013. Šúr, a former late-glacial and Holocene lake at the westernmost margin of the Carpathians. Preslia 85, 239–263.
Płóciennik, M., Self, A., Birks, H.J.B., Brooks, S.J., 2011. Chironomidae (insecta: Diptera) succession in Żabieniec and its palaeo-lake (central Poland) through the late Weichselian and Holocene. Palaeogeogr. Palaeoclimatol. Palaeoecol. 307, 150–167.
Rasmussen, P., Hede, M.U., Noe-Nygaard, N., Clarke, A.L., Vinebrooke, R.D., 2008. Environmental response to the cold climate event 8200 years ago as recorded at Højby Sø, Denmark. Geol. Surv. Den. Greenl. Bull. 15, 57–60.
Rasmussen, S.O., Bigler, M., Blockley, S.P., Blunier, T., Buchardt, S.L., Clausen, H.B., et al., 2014. A stratigraphic framework for abrupt climatic changes during the Last Glacial period based on three synchronized Greenland ice-core records: refining and extending the INTIMATE event stratigraphy. Quat. Sci. Rev. 106, 14–28.
Reille, M., 1992. Pollen et spores d'Europe et d'Afrique du nord. Laboratorie de Botanique Historique et Palynologie, Marseille.
Reimer, P.J., Bard, E., Bayliss, A., Beck, J.W., Blackwell, P.G., Bronk Ramsey, C., et al., 2013. IntCal13 and Marine13 radiocarbon age calibration curves 0–50,000 years cal. BP. Radiocarbon 55 (4), 1869–1887.
Renssen, H., Seppä, H., Crosta, X., Goosse, H., Roche, D.M., 2012. Global characterization of the Holocene thermal maximum. Quat. Sci. Rev. 48, 7–19.
Renssen, H., Isarin, R.F.B., 2001. The two major warming phases of the last deglaciation at 14.7 and 11.5 ka cal BP in Europe: climate reconstructions and AGCM experiments. Glob. Planet. Change 30, 117–153.
Renssen, H., Seppä, H., Heiri, O., Roche, D.M., Goosse, H., Fichefet, T., 2009. The spatial and temporal complexity of the Holocene thermal maximum. Nat. Geosci. 2, 410–413.
Rosén, P., Segerström, U., Eriksson, L., Renberg, I., Birks, H.J.B., 2001. Holocene climatic change reconstructed from diatoms, chironomids, pollen and near-infrared spectroscopy at an alpine lake (Sjuodjijaure) in northern Sweden. Holocene 11 (5), 551–562.
Saunders, K.M., Hodgson, D.A., McMinn, A., 2008. Quantitative relationships between benthic diatom assemblages and water chemistry in Macquarie Island lakes and their potential their potential to reconstruct past environmental changes. Antarct. Sci. 21, 35–49.
Schnitchen, C., Charman, D.J., Magyari, E., Braun, M., Grigorszky, I., Tóthmérész, B., et al., 2006. Reconstructing hydrological variability from testate amoebae analysis in Carpathian peatlands. J. Paleolimnol. 36, 1–17.
Schwark, L., Zink, K., Lechterbeck, J., 2002. Reconstruction of postglacial to early Holocene vegetation history in terrestrial central Europe via cuticular lipid biomarkers and pollen records from lake sediments. Geology 30 (5), 463–466.
Seierstad, I.K., Abbott, P.M., Bigler, M., Blunier, T., Bourne, A.J., Brook, E., et al., 2014. Consistently dated records from the Greenland GRIP, GISP2 and NGRIP ice cores for the past 104 ka reveal regional millennial-scale $\delta^{18}O$ gradients with possible Heinrich event imprint. Quat. Sci. Rev. 106, 29–46.
Seppä, H., Hammarlund, D., Antonsson, K., 2005. Low-frequency and high-frequency changes in temperature and effective humidity during the Holocene in southcentral Sweden: implications for atmospheric and oceanic forcings of climate. Clim. Dyn. 25, 285–297.
Seppä, H., Birks, H.J.B., Giesecke, T., Hammarlund, D., Alenius, T., Antonsson, K., et al., 2007. Spatial structure of the 8200 cal. yr BP event in northern Europe. Clim. Past. 3, 225–236.
Shakesby, R.A., Smith, J.G., Matthews, J.A., Winkler, S., Dresser, P.Q., Bakke, J., et al., 2007. Reconstruction of Holocene glacier history from distal sources: glaciofluvial stream-bank mires and the glaciolacustrine sediment core near Sota Sćter, Breheimen, southern Norway. Holocene 17, 729–745.
Sjögren, P., van Leeuwen, J.F.N., van der Knaap, W.O., van der Borg, K., 2006. The effect of climate variability on pollen productivity, AD 1975/2000, recorded in a Sphagnum peat hummock. Holocene 16 (2), 277–286.
Stone, J.R., Westover, K.S., Cohen, A.S., 2011a. Late Pleistocene paleohydrography and diatom paleoecology of the central basin of Lake Malawi, Africa. Palaeogeogr. Palaeoclimatol. Palaeoecol. 303 (1–4), 51–70.
Stone, J.R., Westover, K.S., Cohen, A.S., 2011b. Late Pleistocene paleohydrography and diatom paleoecology of the central basin of Lake Malawi, Africa. Palaeogeogr. Palaeoclimatol. Palaeoecol. 303, 51–70.
Tamaş, T., Causse, C., 2001. U–Th TIMS chronology of two stalagmites from V11 Cave (Bihor Mountains, Romania). Theor. Appl. Karstol. 13–14, 25–32.
Tátosová, J., Veselý, J., Stuchlík, E., 2006. Holocene subfossil chironomid stratigraphy (Diptera: Chironomidae) in the sediment of Plešné lake (the Bohemian forest, Czech Republic): palaeoenvironmental implications. Biologia 61 (Suppl. 20), 401–411.
ter Braak, C.J.F., Šmilauer, P., 2002. CANOCO Reference Manual and CanoDraw for Windows User's Guide: Software for Canonical Community Ordination (Version 4.5). Biometrics, Wageningen, p. 500.
Tinner, W., Lotter, A.F., 2001. Central European vegetation response to abrupt climate change at 8.2 ka. Geology 29, 551–554.
Tóth, M., Magyari, E.K., Brooks, S.J., Braun, M., Buzckó, K., Bálint, M., Heiri, O., 2012. A chironomid-based reconstruction of late glacial summer temperatures in the southern Carpathians (Romania). Quat. Res. 77, 122–131.
Tóth, M., Magyari, E.K., Buczkó, K., Braun, M., Panagiotopoulos, K., Heiri, O., 2015. Chironomid-inferred Holocene temperature changes in the south Carpathians (Romania). Holocene 25, 569–582.
Väliranta, M., Salonen, J.S., Heikillä, M., Amon, L., Helmens, K., Klimaschewski, A., et al., 2014. Plant macrofossil evidence for an early onset of the Holocene summer thermal maximum in northernmost Europe. Nat. Commun. 6, 6809.
Van der Knaap, W.O., van Leewen, J.F.N., Svitavská-Svobodová, H., Pidek, I.A., Kvavadze, E., Chichinadze, M., et al., 2010. Annual pollen traps reveal the complexity of climatic control on pollen productivity in Europe and the Caucasus. Veg. Hist. Archaeobot. 19, 285–307.
Van der Werff, A., 1955. A new method for cleaning and concentrating diatoms and other organisms. Verhandlungen Int. Ver. für theoretische Angew. Limnol. 12, 276–277.
Van Hardenbroek, M., Heiri, O., Wilhelms, M.F., Lotter, A.F., 2011. How representative are subfossil assemblages of Chironomidae and common benthic invertebrates for the living fauna of Lake De Waay, the Netherlands? Aquat. Sci. 73, 247–259.
Velle, G., Brodersen, K.P., Birks, H.J.B., Willassen, E., 2010. Midges as quantitative temperature indicator species: lessons for palaeoecology. Holocene 20 (6), 989–1002.
Von Grafenstein, U., Erlenkeuser, H., Brauer, A., Jouzel, J., Johnsen, S.J., 1999. A mid-European decadal isotope-climate record from 15,500 to 5000 years BP. Science 284 (5420), 1654–1657.
Walker, M., Johnsen, S., Rasmussen, S.O., Popp, T., Steffensen, J.-P., Gibbard, P., et al., 2009. Formal definition and dating of the GSSP (Global Stratotype Section and Point) for the base of the Holocene using the Greenland NGRIP ice core, and selected auxiliary records. J. Quat. Sci. 24, 3–17.
Walker, M.J.C., Berkelhammer, M., Björck, S., Cwynar, L.C., Fisher, D.A., Long, A.J., et al., 2012. Formal subdivision of the Holocene series/epoch: a discussion paper by a working group of INTIMATE (integration of ice-core, marine and terrestrial records) and the subcommission on quaternary stratigraphy (international commission on stratigraphy). J. Quat. Sci. 27 (7), 649–659.
Wiederholm, T. (Ed.), 1983. Chironomidae of the Holarctic Region. Keys and Diagnoses. Part 1- Larvae. Entomologica Scandinavica. Suppl. 19.
Wiersma, A.P., Renssen, H., 2006. Model–data comparison for the 8.2 ka BP event: confirmation of a forcing mechanism by catastrophic drainage of Laurentide Lakes. Quat. Sci. Rev. 25, 63–88.